NTNU

Norwegian University of
Science and Technology

Flow Transformation in Lower and Upper Turbidite Units, NE Helgeland Basin, Offshore Mid-Norway

Devina Anisa Wikaputri

Natural Resources Management
Submission date: May 2018
Supervisor: Maarten Felix, IGP

Norwegian University of Science and Technology
Department of Geoscience and Petroleum

We judge ourselves by what we feel capable of doing, while others judge us by what we have already done. -Henry Wadsworth Longfellow

Abstract

Sediment transport towards the ocean floor is mainly by sediment gravity flows, either dominated by one flow process such as a slide, slump, debris flow or turbidity current, or more complex flows combining e.g. debris flows and turbidity currents (transitional flows). However, the expected product of a single gravity flow is not straightforward due to the possibility of flow transformation, which allows change of the original flow into a new type. Flow transformation is commonly observed as having a gradual interface between two different sediment gravity flow deposits that formed from different flow types (e.g. debrite and turbidite). Flow transformation has two end-members: (1) dense to dilute flow, and (2) dilute to dense flow, where each consists of a continuum of processes. The resulting deposits often look similar, which can result in misleading interpretation. Therefore, there is a need to study the distinguishing characteristics of the two end-members, which is looked at here.

This research studies the Upper Permian to Lower Triassic Turbidite Units from the NE Helgeland Basin, offshore mid Norway. Two cores, 6611/09-U-01 and 6611/09-U-02, were drilled through these successions. Previous work by Bugge et al. (2002) divided the successions into two units: (1) Lower Turbidite Unit and (2) Upper Turbidite Unit. The objective of this work is to study the depositional processes of these two units, in terms of flow transformation. Facies and facies associations were determined through detailed description of the cored succession and thin section microscopy.

Based on the observations, 14 main lithofacies were defined according to the grain size, texture, and sedimentary structures. The facies were combined into facies associations, showing that the successions include four transitional flow deposits: (1) debrite encased in low density turbidites, (2) alternating dense material and mixed debrite, (3) high density turbidite – debrite couplet, and (4) High density turbidite – debrite – low density turbidite.

Acknowledgement

This thesis titled “Flow Transformation in Co-Genetic Turbidites, NE Helgeland Basin, offshore mid-Norway” was submitted to complete my master’s thesis in Norwegian University of Science and Technology. This thesis took a semester worth of log description and thin section study. And another awfully short semester to complete the writing.

I would like to thank my supervisor, Maarten Felix, for his guidance and patience that has led me to where I am today, completing this thesis and soon my master’s degree (right after the defence!). Maarten is a very good lecturer. He is very approachable and very quick in giving constructive feedback. His enthusiasm inspired me in many ways. He also helped me to participate in my first ever conference, EGU 2018, which was a wonderful experience.

Then I would like to thank my lovely mom and dad, my brother, my sister and my big family in Indonesia for their support and the little updates in their lives that makes me feel close to home, even though we all live in different countries. I miss you. I would also like to thank my other family; Indonesian Student Association (PPIT) and Indonesian families in Trondheim, for creating a home away from home and sharing some of the best moments and adventures in my life.

Last but not least, I would like to thank Vian, for always being just a call away through my ups and downs throughout my master’s study, even with the 6-hour difference in our time zones. You kept my sanity in check during hectic times.

1 TABLE OF CONTENTS

1 INTRODUCTION 1

1.1 Research questions 2

1.2 Methodology 3

2 Background 4

2.1 Geological setting and history 4

2.2 Previous work on the cores 9

2.3 Flow transformation mechanisms and hybrid beds 10

3 Results and interpretation 14

3.1 Facies 14

3.2 Microstructures in mudstone 44

3.3 Sand Injectites 54

3.4 Facies associations and flow models 55

4 Discussion 70

4.1 Dense to dilute flow transformation 70

4.2 Dilute to dense flow transformation 71

4.3 Summary: How to differentiate which type of flow transformation? 73

4.4 Environmental settings 76

5 Conclusion 77

Fig. 1: Geological setting of Trøndelag Platform and Helgeland Basin. Both well 6611/09-U-01 and 6611/09-U-02 were drilled close to the coast of mid-Norway. Structural elements defined by NPD. From Hallan et al. (2014). 5
Fig. 2: Lithostratigraphic column of the study area based on work by Bugge et al., (2002) 6
Fig. 3: Tectonic history of the study area in (a) Late Permian transgression event shown by the blue arrows, and (b) Early Triassic. From Doré (1991). 8
Fig. 4: Diagrams showing (a) flow and deposit models for dense to dilute flow transformation according to the material strength, which progressively decreases from top to bottom (from Felix et al., 2009); (b) flow run out models of (1) normal turbidity current, and (2) dilute to dense transforming flow (from Haughton et al., 2009); and (c) the idealised sequence of deposits formed by the dilute to dense transforming flow (from Haughton et al., 2009),..... 11
Fig. 5: Injection and delamination mechanism (Fonnesu et al., 2016) 13
Fig. 6: Core photos showing conglomerate facies (a) erosional lower contact in contact with the massive sandstone facies and slightly coarsening upward trend to the top (from core 6611/09-U-01, depth interval 322 m – 322 m), (b) upper contact of the conglomerate facies fining upwards into massive sandstone (from core 6611/09-U-01, depth interval 200 m – 201 m). The depth intervals are measure from top downward for each 1 metre long core, measurement on the side of the photos indicate 10 cm intervals downward (1 – 100 cm)... 16
Fig. 7: Core photos showing massive sandstone facies, (a) lower contact with load and flame structures into mudstone (from core 6611/09-U-01, depth interval 100 m – 101 m), (b) interval of thick massive sandstone bed showing a gradual upper contact with fining upward sandstone (from core 6611/09-U-02, depth interval 22 m – 23 m). The depth intervals are measure from top downward for each 1 metre long core, measurement on the side of the photos indicate 10 cm intervals downward (1 – 100 cm). 18
Fig. 8: Core photos showing patchy sandstone facies, (a) rounded pockets of fine sand within very coarse, massive- sandstone (from core 6611/09-U-01, depth interval 14 m – 15 m), (b) elongated and distorted sand patches with varying grain sizes within very coarse, massive sandstone (from core 6611/09-U-01, depth interval 33 m – 34 m). Red arrows point to the sand patches. The depth intervals are measure from top downward for each 1 metre long core, measurement on the side of the photos indicate 10 cm intervals downward (1 – 100 cm). 20

Fig. 9: Core photos showing coarsening upward sandstone facies that transition to fining upward facies, (a) gradual coarsening up from massive sandstone (from core 6611/09-U-02, depth interval 164 m – 165 m), (b) thin coarsening upward bed at the base of a turbidite (from core 6611/09-U-02 depth interval 277 m – 278 m). The depth intervals are measure from top downward for each 1 metre long core, measurement on the side of the photos indicate 10 cm intervals downward (1 – 100 cm). 22
Fig. 10: Core photos showing fining upward sandstone facies in a turbidite facies association, (a) fining upwards into parallel laminated sandstone (from core 6611/09-U-02, depth interval 83 m – 84 m), (b) fining upwards sandstone with Bouma B, C and E (from core 6611/09-U-01, depth interval 141 m – 142 m). The depth intervals are measure from top downward for each 1 metre long core, measurement on the side of the photos indicate 10 cm intervals downward (1 – 100 cm)..... 24
Fig. 11: Core photos showing two types of planar laminated sandstone, (a) thick bed (>30 cm) showing planar-laminated sandstone (from core 6611/09-U-01, depth interval 301 m – 302 m), (b) red box showing thin (<10cm) planar-laminated sandstone with erosive base (from core 6611/09-U-02, depth interval 91 m – 92 m). The depth intervals are measure from top downward for each 1 metre long core, measurement on the side of the photos indicate 10 cm intervals downward (1 – 100 cm). 26
Fig. 12: Core photos showing different variation of distorted heterolithic beds, (a) muddy distorted beds with sharp lower and gradual upper contact into chaotic sandstone facies (from core 6611/09-U-02, depth interval 230 m -231 m), (b) sandy distorted bed encased in a massive sandstone with sharp upper and lower contacts (from core 6611/09-U-02, depth interval 244 m -245 m). The depth intervals are measure from top downward for each 1 metre long core, measurement on the side of the photos indicate 10 cm intervals downward (1 – 100 cm). 28
Fig. 13: Core photos showing chaotic facies with floating mud clasts, (a) gradual lower contact from muddy sandstone into chaotic facies with the randomly oriented mud clasts (from core 6611/09-U-02, depth interval 42 m -43 m), (b) slightly oriented clasts with the bigger clasts near to the base of the bed (from core 6611/09-U-02, depth interval 92 m -93 m). The depth intervals are measure from top downward for each 1 metre long core, measurement on the side of the photos indicate 10 cm intervals downward (1 – 100 cm)... 30

Fig. 14: Core photos of very thin ripple sandstone facies pointed at by the red arrows (a) ripples in a typical Bouma sequence (as Bouma T_c) with gradual lower contact with planar laminated sandstone (from core 6611/09-U-02, depth interval 160 m -161 m), (b) sequences of low density turbidites consisting of planar laminated sandstone, ripple sandstone, and massive mudstone (from core 6611/09-U-02, depth interval 272 m -273 m). The depth intervals are measure from top downward for each 1 metre long core, measurement on the side of the photos indicate 10 cm intervals downward (1 – 100 cm). 32
Fig. 15: Core photos showing loaded ripple, (a) very thin sandstone bed loading into the mud with vague ripple internal structures, thus they look like lenticular beds (from core 6611/09-U-01, depth interval 88 m -89 m), (b) very thin sandstone with clearer ripple structures, loading is more apparent at the upper part of this interval (from core 6611/09-U-02, depth interval 148 m -149 m). The depth intervals are measure from top downward for each 1 metre long core, measurement on the side of the photos indicate 10 cm intervals downward (1 – 100 cm). 34
Fig. 16: Core photos showing the thinly layered interbedded sandstone and mudstone, (a) very thin layers of this facies with gradual contact and fining up sequences (from core 6611/09-U-01, depth interval 176 m - 177), (b) alternating mudstone-sandstone with sharp lower and upper contacts, the more wavy contact indicates loading or rippled structure (from core 6611/09-U-02, depth interval 198 m -199 m). The depth intervals are measure from top downward for each 1 metre long core, measurement on the side of the photos indicate 10 cm intervals downward (1 – 100 cm). 35
Fig. 17: Core photos showing muddy sandstone facies (a) thin bedded muddy sandstone (from core 6611/09-U-01, depth interval 307 m -308 m), (b) thick bedded muddy sandstone with large mud clasts (from core 6611/09-U-02, depth interval 255 m -256 m). The depth intervals are measure from top downward for each 1 metre long core, measurement on the side of the photos indicate 10 cm intervals downward (1 – 100 cm). 37
Fig. 18: Core photos showing sandy mudstone facies with floating sand grains and pebbles (a) from core 6611/09-U-02, depth interval 220 m - 221 m, (b) from core 6611/09-U-02, depth interval 255 m -256 m. The depth intervals are measure from top downward for each 1 metre long core, measurement on the side of the photos indicate 10 cm intervals downward (1 – 100 cm)..... 39

Fig. 19: Core photos showing laminated mudstone (a) from core 6611/09-U-02, depth interval 183 m - 184 m, (b) from core 6611/09-U-02, depth interval 252 m -253 m. The depth intervals are measure from top downward for each 1 metre long core, measurement on the side of the photos indicate 10 cm intervals downward (1 – 100 cm). 41
Fig. 20: Core photos showing massive mudstone, (a) upper contact is sharp, often preserved loading and flame structure or erosional contact (from core 6611/09-U-02, depth interval 176 m – 177 m), (b) gradual lower contact with laminated mudstone, with few blobs of very thin sandstone encased in the mud, possibly from loading (from core 6611/09-U-02, depth interval 186 m – 187 m). The depth intervals are measure from top downward for each 1 metre long core, measurement on the side of the photos indicate 10 cm intervals downward (1 – 100 cm). 43
Fig. 21: Laminated mudstone that shows silt ripples (a) core photo of the dark grey laminated mudstone (depth interval 133.27 m – 133.32 m), (b) full thin section scan, (c) with magnification of 5x , field of view is 3.6 mm, (d) discontinuous, lenticular silt layers pointed at by the arrows. 45
Fig. 22: Laminated mudstone that shows silt ripples, interlaminated with massive sandstone (a) core photo of the section (depth interval 161.6 m – 161.65 m), (b) full thin section scan, (c) with magnification of 5x, field of view = 3.6 mm, (d) discontinuous, lenticular silt layers pointed at by the arrows. 46
Fig. 23: Calciturbidites, interlaminated mudstone and calcareous fossil rich layers (a) core photo of the section (depth interval 213.1 m – 213.15 m), (b) full thin section scan, (c) shell fragment and ooids pointed at by the arrows, with magnification of 5x, field of view = 3.6 mm, (d) interbedded mud and fossil rich layers. 48
Fig. 24: Parallel laminated mudstone composed of interlaminated silt layers and fine silt/clay layers (a) core photo of the section (depth interval 274.6 m – 274.65 m), (b) full thin section scan, (c) parallel interlaminations with magnification of 5x, field of view = 3.6 mm, (d) a subtle fining upward from coarse silt into fine silt pointed by the arrow. 49
Fig. 25: Parallel laminated mudstone composed of interlaminated silt layers and fine silt/clay layers (a) core photo of the section (depth interval 274.6 m – 274.65 m); above the white arrow is a loading structure, (b) full thin section scan, (c) parallel interlaminations with magnification of 5x, field of view = 3.6 mm, (d) zoomed in version of the mud lamina. 51

Fig. 26: Inhomogeneous mudstone showing discontinuous silt and mud layers (a) a core photo of the section (depth interval 64.7 m – 64.75 m), (b) full thin section scan, (c) inhomogeneous mudstone with magnification of 5x, field of view = 3.6 mm, (d) a silty, discontinuous lamina, with some fine materials below and above it. 52
Fig. 27: Inhomogeneous mudstone showing discontinuous silt and mud layers (a) a core photo of the section (depth interval 182.2 m – 182.25 m), (b) full thin section scan, (c) inhomogeneous mudstone with magnification of 5x, field of view = 3.6 mm, (d) a silty, discontinuous lamina, with some fine materials below and above it. 53
Fig. 28: Core photo showing sand injectite of medium sandstone intruding into interbedded sandstone-mudstone interval. The contact with the host bed is discordant and wavy. From core 6611/09-U-02, depth interval 270 m – 271 m. The depth intervals are measure from top downward for each 1 metre long core, measurement on the side of the photos indicate 10 cm intervals downward (1 – 100 cm). 54
Fig. 29: Diagram showing the facies association and flow process of a low-density turbidity current. 55
Fig. 30: Core photos showing facies association of a low density turbidite. 56
Fig. 31: Diagram showing the facies association and flow process of a high-density turbidity current. 57
Fig. 32: Core photos showing facies association of a high density turbidite. Core photos showing the whole 1 metre section where the facies association occurred. 58
Fig. 33: Diagram showing the facies association and inferred flow process of a mud flow. ... 59
Fig. 34: Diagram showing the facies association and inferred flow process of a debris flow. 60
Fig. 35: Diagram showing the facies association and inferred flow process of a slump. 61
Fig. 36: Diagram showing the facies association and inferred flow process of a slide. 61
Fig. 37: Core photos showing facies associations of slump and slide. 62
Fig. 38: Diagram showing the facies association and inferred flow process of a dense to dilute flow transformation 63
Fig. 39: Diagram showing the facies association and inferred flow process of a dense to dilute flow transformation 64
Fig. 40: Core photos showing facies association of a debrite encased in low density turbidite (LDT). 65

Fig. 41: Core photos showing facies association of alternating dense material and mixed debrite. Core photos showing the whole 1 metre section where the facies association occurred..... 66
Fig. 42: Diagram showing the facies association and inferred flow process of a dilute to dense flow transformation 67
Fig. 43: Diagram showing the facies association and inferred flow process of a dilute to dense flow transformation 68
Fig. 44: Core photos showing facies association of debrite underlain by massive sandstone (high density turbidite/HDT) and overlain by low density turbidite (LDT) 69
Fig. 45: Summary of the different stages in both end-members of the flow transformation. The blue boxes and arrow show dense to dilute flow transformation, while the pink boxes and arrow show dilute to dense flow transformation. The boxes showing common flow transformations in bold, and the expected deposits in the brackets. LDT = low density turbidity, HDT = high density turbidite, LDTC = low density turbidity current, HDTC = high density turbidity current. 74
Fig. 46: Summary of the deposit characteristics of the two end-members of the flow transformation. Blue arrow shows dense to dilute flow transformation, and pink arrow shows dilute to dense flow transformation. 75

1 INTRODUCTION

For decades, understanding sediment gravity flows was mostly through study of ancient deposits (outcrops, cores) and controlled laboratory experiments, which resulted in numerous classifications and models, e.g. Bouma Sequence (Pickering et al. 2016) and Lowe Sequence (Lowe, 1982). The product of a single gravity flow is however not straightforward due to the possibility of flow transformation, that is the change from one flow type to another (e.g. Haughton et al., 2003; Talling et al., 2004; Amy & Talling, 2006; Felix & Peakall, 2006; Felix et al., 2009; Haughton et al., 2009). A single sediment gravity flow also has the possibility to undergo more than one flow transformation throughout its flow history.

Based on previous studies of ancient deposits and laboratory experiments, flow transformation has two end-members: (1) from dense flow to dilute flow, and (2) from dilute flow to dense flow. The former was suggested in the early years of sediment gravity flow study, while the latter was introduced later on and is relatively new. The transformation of dense flow into dilute flow (e.g. debris flow into turbidity current) has been inferred to occur via different dilution mechanisms. The efficiency of these dilution mechanisms has also been described by Felix & Peakall (2006) in their laboratory experiment. On the other hand, the transformation of dilute to dense flow have been studied extensively via outcrop studies which shows the lateral extent of the transformation. For example, a turbidity current can transform into a debris flow through turbulence damping by the entrainment of cohesive clay particles and subsequent flow deceleration (e.g. Talling et al., 2004; Haughton et al., 2009).

Although both end-members have been studied and described extensively, there's a lack in the correlation to the overall flow transformation spectrum; that the transformation can go one way or another and different stages of the transformation can look very similar in the deposits. It is difficult to tell which flow transformation took place as the same flow process can result in distinctly different deposits. In contrast, different flow process can result in similar deposits. Without a clear difference, the interpretation of the deposits can be misleading. Therefore, there is a need to establish a set of distinguishing characteristics to tell the two end members of flow transformation apart.

1.1 RESEARCH QUESTIONS

Flow transformation is inferred to occur as one parental flow that can change its flow regime (e.g. by bulking up, Haughton et al., 2009) or it can also occur from the segregation of the parental flow into separate parts (e.g. as a dense mass and turbid cloud, Felix & Peakall, 2006). The transformation is commonly observed as a gradual interface between two different sediment gravity flow deposit types (e.g. debrite and turbidite). Regardless of the flow process, the study of flow transformation from the ancient deposits can be very tricky as the interface can also be sharp and conformable to normal bedding. In this work, where both (1) dense to dilute, and (2) dilute to dense flow transformation have occurred, it is often difficult to differentiate which transformation the parent flow has undergone because the deposits from each end-member can look very similar. Therefore, the main aim of this research is to (attempt to) deduce the identifying characteristics of each flow transformation end members.

This research used two shallow stratigraphic cores, 6611/09-U-01 and 6611/09-U-02, that were drilled on the Trøndelag Platform, just offshore from the Norwegian mainland (Fig. 1). The two wells penetrated Upper Permian to Lower Triassic sediments with 60 m stratigraphic overlap (Bugge et al., 2002). The studied intervals include the Lower and Upper Turbidite Units from both cores and they consist of beds that are more complex than what Bugge et al. (2002) have described in their paper as massive and fining upward turbidites and slumps.

In addition, the mud portion of the Turbidite Units will be described in some more detail based on a study of thin sections to identify microstructures within the laminated or seemingly massive mudstones.

1.2 METHODOLOGY

Detailed observations of the cores were recorded on a logging sheet with 1:20 scale. The grain size of each bed is determined using a hand lens and a grain size comparator. The core has been cut in half and stored in section, where each core section is a metre in length. Depth is measured from the top downwards. The first 10 m of 6611/09-U-01 and 8 m from 6611/09-U-02 were part of the Quaternary overburden rock, and are not included in the cores. In total, 629 m of cores were described as part of:

- Lower Turbidite Unit: 166 m from 6611/09-U-01 (depths 202 m until 368 m).
- Upper Turbidite Unit: 191 m from 6611/09-U-01 (depths 11 m until 202 m) and 272 m from 6611/09-U-02 (depths 8 m until 281).

Facies and facies association analyses were carried out based on the observations. The facies association is then used to interpret the flow process. In addition, thin sections of selected interval of the cores were also used to observe mud microstructures. The thin sections used were part of core(s):

- 6611/09-U-01, depth 213.1 m – laminated mudstone
- 6611/09-U-01, depth 253.7 m – massive mudstone
- 6611/09-U-02, depth 64.7 m – massive mudstone
- 6611/09-U-02, depth 133.27 m – laminated mudstone
- 6611/09-U-02, depth 161.6 m – laminated mudstone
- 6611/09-U-02, depth 182.2 m – massive mudstone
- 6611/09-U-02, depth 274.6 m – laminated mudstone

2 BACKGROUND

2.1 GEOLOGICAL SETTING AND HISTORY

The Trøndelag Platform is situated off the Norwegian mainland, bounded by a series of structural highs to the northwest, and by the Froan Basin and the Frøya High to the southwest (Fig. 1). The evolution of the Norwegian continental shelf and seaways was heavily influenced by the Caledonian orogeny that lasted until the Devonian. The Caledonian orogeny marks the closing of the Iapetus Ocean and the collision of the Laurentian and Baltic plates. The resulting Iapetus suture lies offshore between East Greenland and mid-Norway with a NE-SW trend (Doré, 1991). Previous work on these cores by Bugge et al. (2002) correlated most of the rocks to the East Greenland formations; Fig. 2 shows the stratigraphic column of the study area based on this work.

Preceding the Caledonian orogeny, the Variscan orogeny (present day North Sea) and the Uralian orogeny (present day Barents Sea) events superimposed the newly formed Pangea supercontinent throughout the Late Palaeozoic/Carboniferous until the earliest Triassic. In result, a complex basement anisotropy was created (Doré, 1991). Active shear zones bounded some of the Devonian basins, such as the Hitra Fault Alignment (Fig. 3). Post orogenic events include multistage rifting and crustal thinning of the NE Atlantic region that resulted in many rotated fault blocks beneath the Trøndelag Platform in the Late Carboniferous to Early Permian as revealed by deep seismic reflection data (Doré, 1991; Osmundsen et al., 2002; Faleide et al., 2010).

Devonian to Carboniferous

After the culmination of the Caledonian mountain belt, the rest of Devonian saw the development of an intermontane basin that was filled by continental red beds (Surlyk et al., 1986). Major faults bounded the Devonian basin that was part of the N-S trending folds and thrusts. This depositional setting continued until the Carboniferous. In the Late-Carboniferous, a new rifting phase began causing the formation of the Norwegian-Greenland Sea (ca. 300 ma) as revealed from northern East Greenland (Surlyk et al., 1986; Faleide et al., 2010).

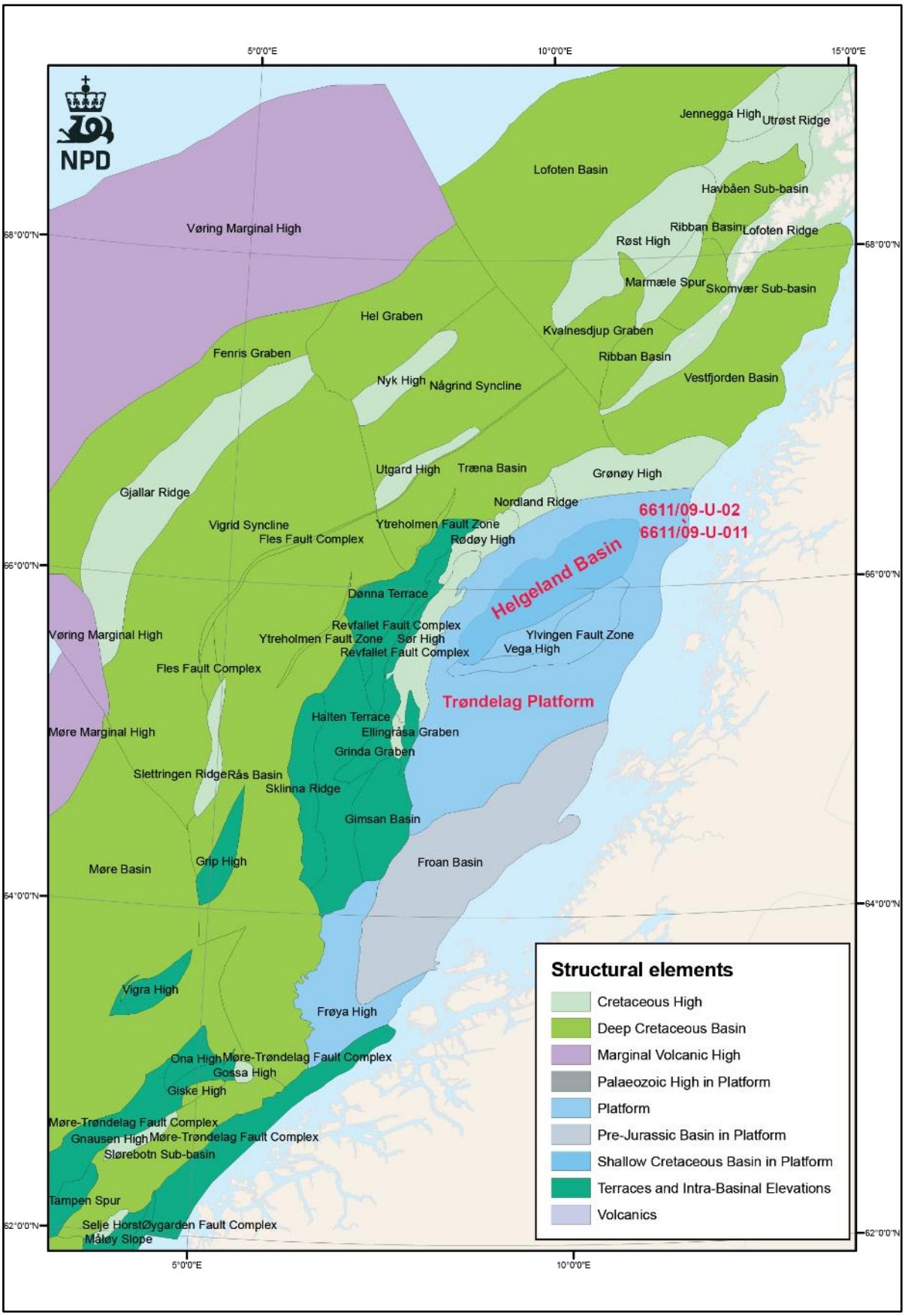

Fig. 1: Geological setting of Trøndelag Platform and Helgeland Basin. Both well 6611/09-U-01 and 6611/09-U-02 were drilled close to the coast of mid-Norway. Structural elements defined by NPD. From Hallan et al. (2014).

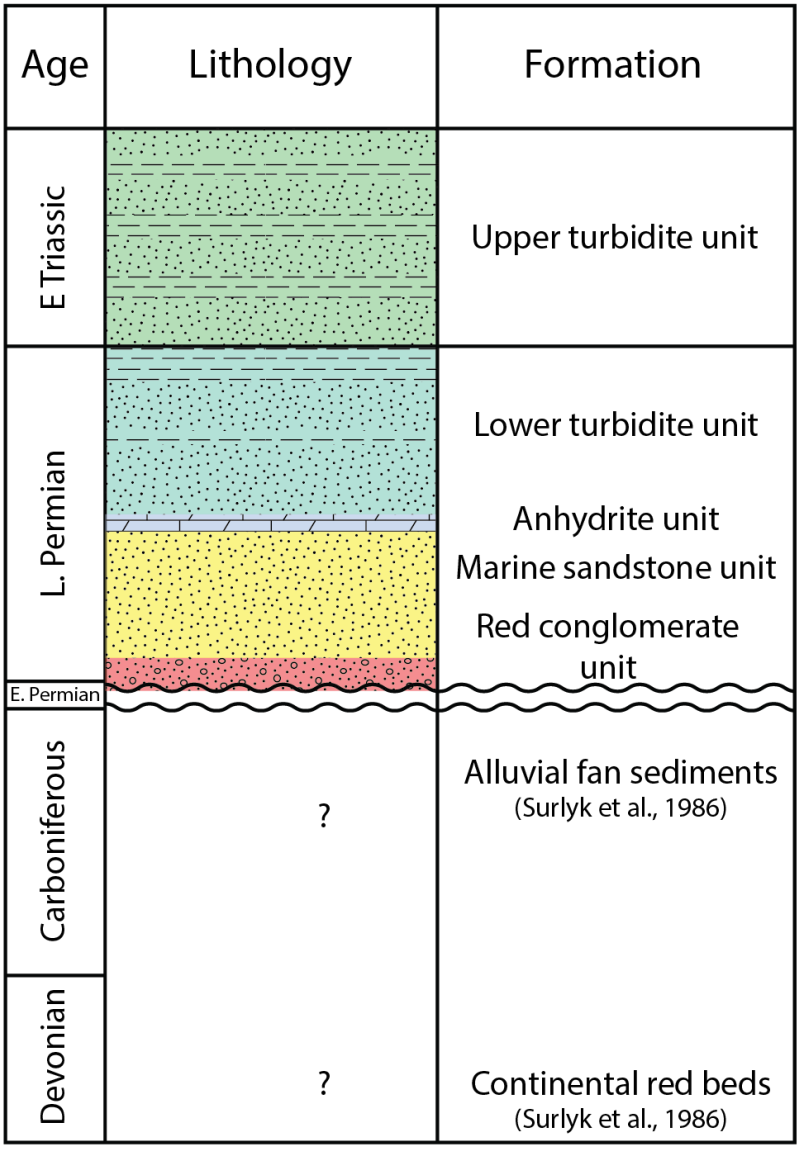

Fig. 2: Lithostratigraphic column of the study area based on work by Bugge et al., (2002)

Permian to Early Triassic

The rifting lasted until the Early Permian (Faleide et al., 2010), then tilting, uplift and subsequent erosion occurred throughout the Permian. Synchronous basin subsidence and transgression caused by post-rift thermal contraction occurred in the seaway between Greenland and Norway (Surlyk et al., 1986). The overall transgression was intermittent with several regressive events during which red/brown conglomeratic beds of the Huledal Fm. were deposited (Surlyk et al., 1986). Bugge et al. (2002) correlated this formation with the lowermost Permian unit from the 6611/09-U-01 cores. The Late Permian transgression covered the whole area of the Atlantic Rift Domain (blue arrows in Fig. 3a), during which the

organic-carbon-rich shales of the Ravnefjeld Fm. were deposited. By the Early Triassic, marine incursions from the Boreal and Tethys Oceans brought marine condition that deposited the Wordie Creek Fm (Fig. 3b). (Doré, 1991).

In summary, the study area at the time of deposition formed narrow basin located in the graben that was tilted as the result of several rifting episodes between mainland Norway and Greenland. The depositional environment changed from mainly alluvial-fan continental deposits into deep marine deposits as the result of Late Permian-Early Triassic transgression. By the Early Triassic, most of the basins near the Norwegian mainland were NW dipping half-grabens with normal faults that have SE trending throws, at this time most of the faults had become inactive. Subsequently, the Middle Triassic and younger sediments filled in the basin and their deposits are more gently dipping compared to the older sediments (Osmundsen et al., 2002).

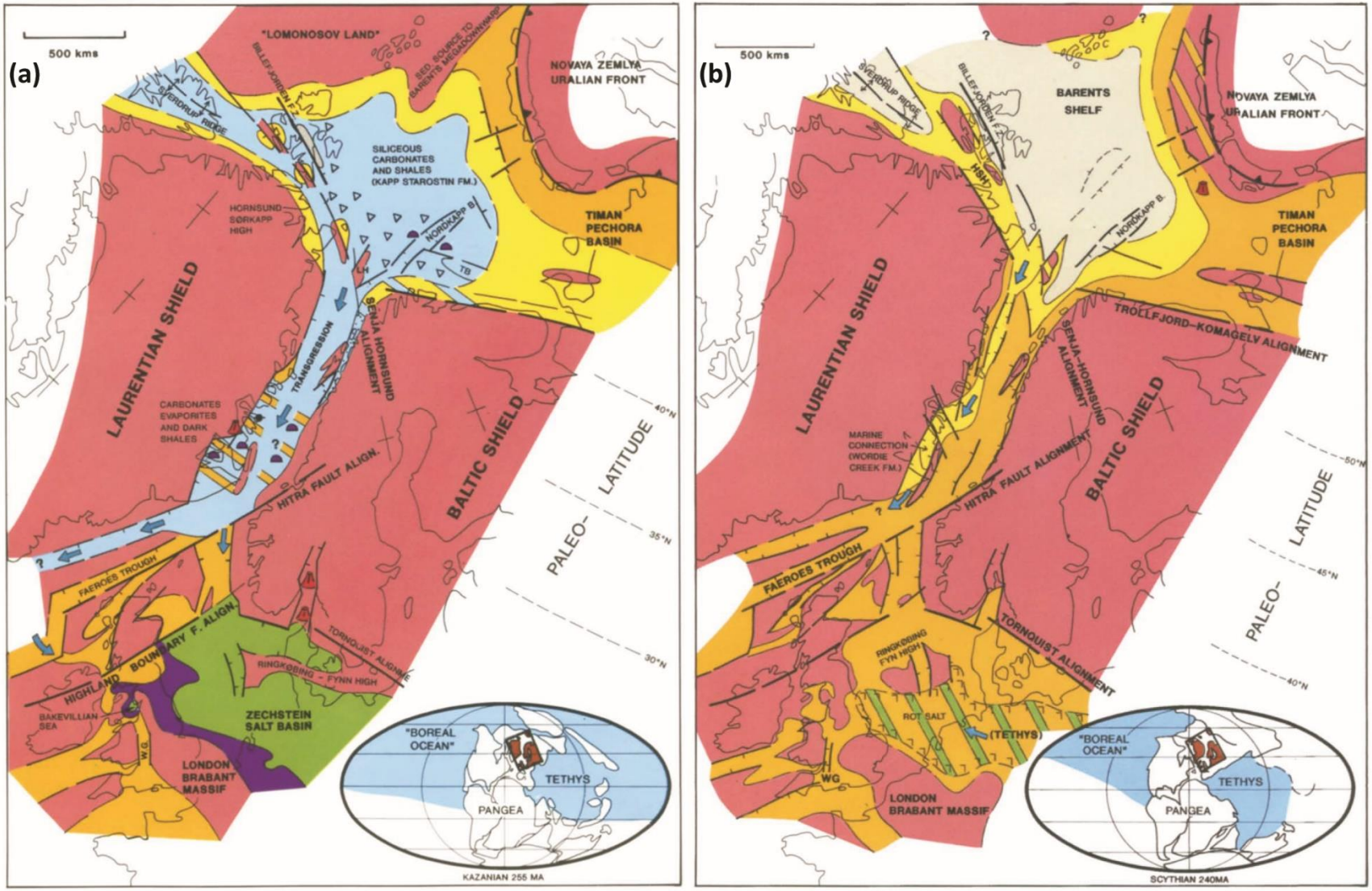

Fig. 3: Tectonic history of the study area in (a) Late Permian transgression event shown by the blue arrows, and (b) Early Triassic. From Doré (1991).

2.2 PREVIOUS WORK ON THE CORES

Bugge et al. (2002) divided the cored succession into four units: Shallow Marine Sandstone Unit, Anhydrite Unit, Lower and Upper Turbidite Units (Fig. 2). The lowest 174.5 m are made up of massive, shallow marine sandstones overlain the conglomerates with an abrupt change. Bioturbation is very common and contributes to the homogenisation of the sand. Overall, this unit fines up to laminations of fine grained grey sandstone and weakly bioturbated, red sandstone. This unit is interpreted to have been deposited in an alluvial fan to shoreface environment (Bugge et al., 2002).

Above the Shallow Marine Sandstone Unit lies the 15.5 m thick Anhydrite Unit, which consists of anhydrite-filled fractures in massive sandstone and replacive anhydrite nodules (Bugge et al., 2002). The nodules have a mosaic structures resembling chicken-wire structure. Thus, this unit is interpreted as reworked sabkha or tidal flat anhydrites (Bugge et al., 2002).

The succession continues into the Permian Lower Turbidite Unit with a thickness of 166 m. This unit is described as having 2 parts: successions of complete or parts of Bouma sequence T_a to T_e, organic-rich mudstones and siltstone interbedded with massive sandstone (Bugge et al., 2002). The boundary between the Lower and Upper Turbidite Units is the Permian-Triassic boundary. The Upper Turbidite Unit contains a similar lithology as the Lower Turbidite Unit but is overall finer-grained with a higher occurrence of high density turbidites (Bugge et al., 2002). Both Turbidite Units are interpreted as the result of episodic gravity flows proximal to a slope indicated by an abundance of terrestrial palynofacies (Bugge et al., 2002). The work concluded that both the Lower and Upper Turbidite Units were the result of two single flow processes: turbidity currents and slumps from tectonically induced slope failures.

2.3 FLOW TRANSFORMATION MECHANISMS AND HYBRID BEDS

Flow transformation is commonly observed between debris flow (dense) and turbidity current (dilute). The resulting deposits of dense to dilute flow transformation are normally classified as hybrid event beds, or linked debrites (Haughton et al., 2003; Talling et al., 2004; Amy & Talling, 2006; Haughton et al., 2009). The vertical relationship between the beds (i.e. debrite and turbidite) is important as it tells the type of depositional mechanism as well as any indication of flow transformation. The progressive change of the parent flow will be recorded in the deposits as different stages of flow transformation. Each stage is the result of one or more flow transformation mechanisms. A single flow transformation can have different mechanisms according to the vertical and lateral position within the flow. The mechanisms of the two end-members, dense to dilute flow and dilute to dense flow transformation, have been discussed based on laboratory experiments, core descriptions, and extensive outcrop studies (Haughton et al., 2003; Talling et al., 2004; Amy & Talling, 2006; Felix & Peakall, 2006; Felix et al., 2009).

In general, the transformation from dense to dilute flow incorporates a dilution mechanism. The mechanisms for dense to dilute transformation depends on the material strength and the composition of the initial parent flow, because it largely affects the extent of mixing and/or dilution (Felix & Peakall, 2006; Felix et al., 2009). The material strength affects the deformability of the dense flow, e.g. erosion at the top of the dense material (Felix & Peakall, 2006), and thus the efficiency of the dilution mechanism. An efficient transformation means most of the dense material is incorporated to the transforming flow. A lower material strength means more erosion and mixing of the dense flow at the interface with the overlying turbulent cloud resulting from the erosion of the dense flow. In contrast, a dense flow with a higher material strength would then have little to no erosion at the interface and remains unmixed. Because of the inefficient transformation, such a dense flow is deposited as a normal slump or debrite.

The mechanisms for dense to dilute flow transformation are shown in Fig. 4a, in order of progressive transformation (i.e. less mixing to more mixing), which include: erosion from the interface between the dense mass and the turbid cloud, erosion of the wavy interface between the dense mass and turbid cloud; breaking of the dense mass (broken

apart flow), breaking of internal waves and fully mixed flow (Felix & Peakall, 2006). Essentially, the dense flow undergoes dilution as the dense material is broken down and subsequently reduces in size.

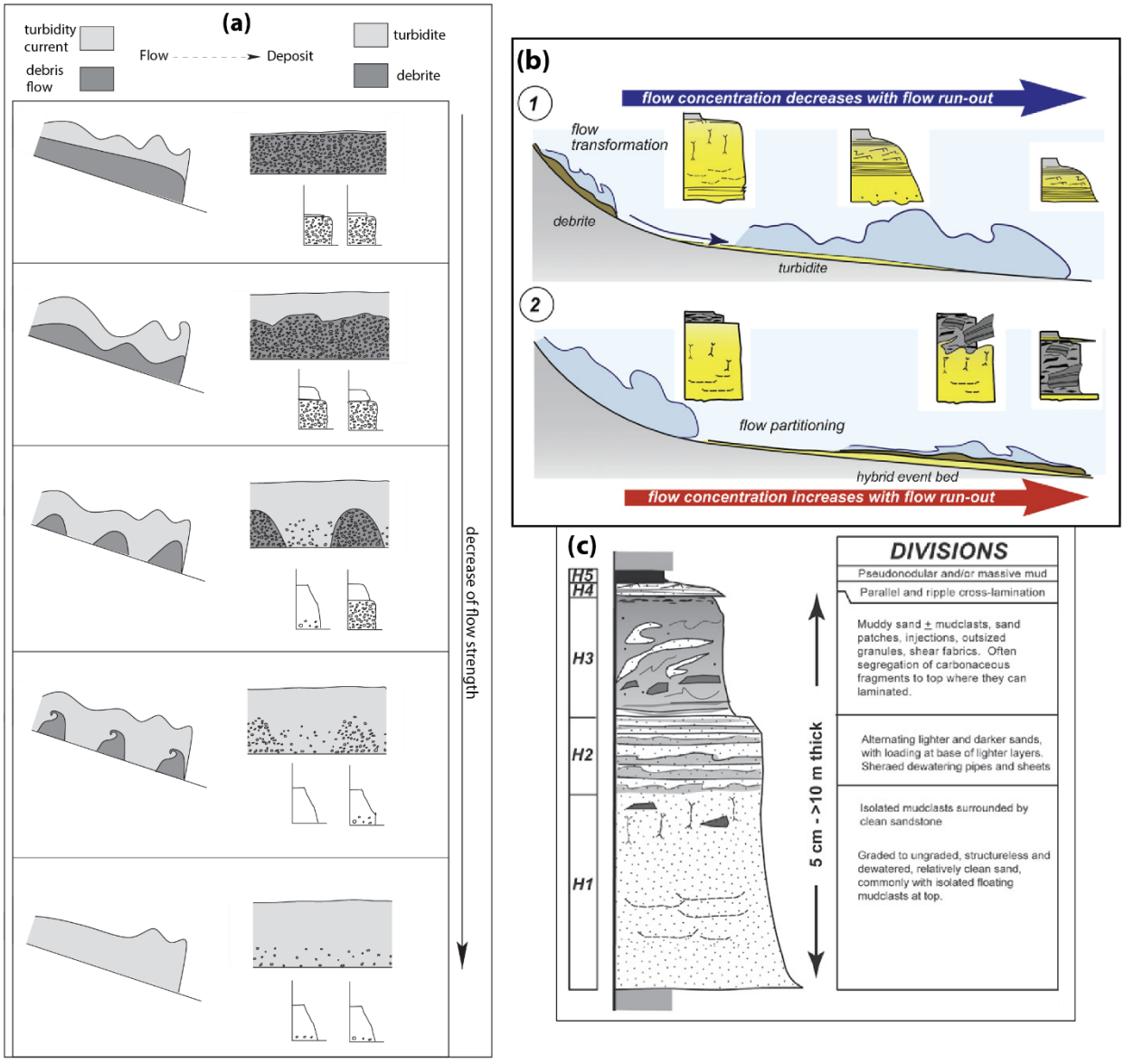

Fig. 4: Diagrams showing (a) flow and deposit models for dense to dilute flow transformation according to the material strength, which progressively decreases from top to bottom (from Felix et al., 2009); (b) flow run out models of (1) normal turbidity current, and (2) dilute to dense transforming flow (from Haughton et al., 2009); and (c) the idealised sequence of deposits formed by the dilute to dense transforming flow (from Haughton et al., 2009),

The opposite is expected to happen in a dilute to dense flow transformation, where the dilute parent flow incorporates clay particles into the flow. There have been several outcrop and core studies that found gradual transitions from turbiditic facies into debritic facies within the distal section of the basin. Such deposits are often called “linked-debrites”

or “hybrid event beds” (Haughton et al., 2003; Talling et al., 2004; Amy & Talling, 2006; Fonnesu et al., 2016). The main interpreted mechanism is by the erosion and incorporation of cohesive particles. For example, an increase in slope combined with converging flow can cause acceleration that enhances erosion of the seabed. Haughton et al. (2003) suggested this mechanism happens on the slopes up-dip where canyons are commonly found. When the turbidity current decelerates (e.g. decrease in slope), the incorporated muddy seabed, provided that it breaks up into dispersed mud, can cause flow partitioning. Flow partitioning occur when the mud-rich part of the flow lags behind the main turbidity current. This results in the deposition of the debritic facies on top of the turbiditic facies as depicted in Fig. 4b picture number 2 (Haughton et al., 2009). Fig. 4 shows a comparison between a normal decelerating turbidity current which decreases its concentration as the flow runs out and a hybrid flow which increases its concentration as the flow runs out.

An experiment by Baas et al. (2009) has shown that the effect of cohesive clay particle incorporation into the flow is the damping of turbulence that subsequently changes the flow regime from turbulent into transitional or laminar flow. Therefore, erosion and disintegration of mud clasts into clay particles causes flow transformation. The damping of turbulence is effective at velocities below ~0.5 ms^{-1}, because high dispersed clay concentration in conjunction with low velocity increase the chance of flocculation (Baas et al., 2009). Baas et al. (2009) also mentioned that there is a higher chance of turbulence damping in the natural system than in laboratory experiments because of the likely presence of clay minerals other than the kaolinite used in the experiment, which has lower cohesive strength than e.g. smectite. The amount of dispersed clay needed is also relatively low, and can result from a shallow erosion in order of tens of cm (Talling et al., 2004). In principle, incorporation of dispersed mud followed by deceleration of the flow can indeed deposit a gradual transition from turbiditic facies in to debritic facies (Haughton et al., 2003; Talling et al., 2004; Amy & Talling, 2006; Haughton et al., 2009; Talling, 2013).

The ‘ideal’ deposits from dilute to dense flow transformation has been classified by Haughton et al., (2009) and comprises of 5 divisions as shown in Fig. 4c as: clean sandstone with or without structures and often floating mud clasts (H1), alternating lighter and darker sand (H2), muddy sandstone (H3), parallel and ripple cross-lamination (H4), and massive mud (H5).

Fonnesu et al. (2016) suggested another mechanism to generate hybrid event beds (dilute to dense flow transformation), that is by the injection and subsequent delamination of large substrate rafts from 2 to 20 meters long. This mechanism occur in distal parts of the basin. The delamination happens at the base of a high density, sandy flows as shown in Fig. 5. The eroded substrate is then transported on top of the high-density flow for a short distance where it starts to break down and become sheared (Fonnesu et al., 2016).

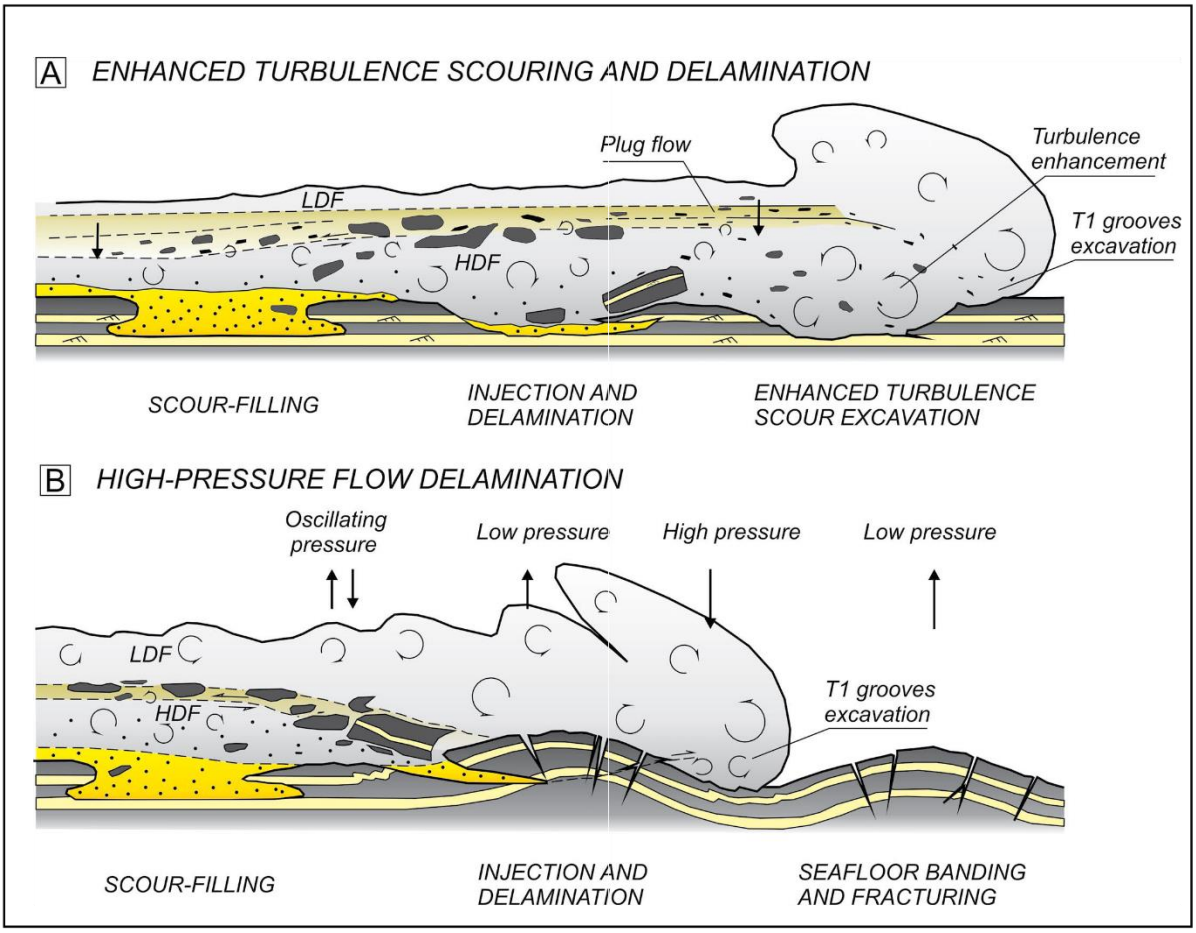

Fig. 5: Injection and delamination mechanism (Fonnesu et al., 2016)

3 RESULTS AND INTERPRETATION

Sedimentological parameters that were analysed include grain characteristics and sorting; bedding thickness and fabric; sedimentary and post-depositional structures; and the nature of upper and lower contacts. Grain characteristics include grain size and sphericity. The thicknesses of the beds are classified in ascending order of thickness as: laminae for less than 1 cm; very thin beds for 1 to 3 cm; thin beds for 3 to 10 cm; medium beds for 10 to 30 cm and thick beds for 30 to 100 cm (Collinson et al. 2006). The fabrics of each bed along with the observed sedimentary structures were used to determine the facies. Each facies represents similar depositional process. Vertical relationships between the facies are expressed by the bedding contacts that are the lower and upper contacts which can either be gradual or sharp. These contacts are important in determining the facies associations as explained further in Section 3.4.

3.1 FACIES

Facies is defined here as an interval within the core that exhibits similar sedimentological parameters. The succession is divided into 14 facies where the grain support and depositional mechanisms are interpreted for each facies.

Conglomerate facies

Description

The conglomerate facies represents the coarsest fraction within the core succession. This facies consists of grain-supported, granules to coarse pebbles with diverse types of clasts. Grain roundness is variable, well-rounded and angular grains can exist in the same bed. Angular mud clasts (2 – 4 cm) are randomly dispersed throughout this facies. The conglomerates are generally very poorly sorted (Fig. 6), massive and thicker than the other facies. The thickness of this facies is commonly 70 to 100 cm. The lower contact is mostly sharp and erosional (Fig. 6a) overlying massive sandstone facies. Occasionally, the lower contact has a gradual coarsening upward part (Fig. 6a). The upper contact is gradual with a fining upward trend into the massive sandstone facies (Fig. 6b).

Interpretation

The larger particles in this facies is supported by the buoyant lift provided by the matrix strength (Lowe, 1979; Lowe, 1982).The depositional mechanism of this facies is by en masse freezing, thus the structureless fabric. Slight coarsening upward at the base may be cause by grain collisions that produce dispersive pressure. Conglomerates are commonly found in a debris flow (Lowe, 1979)

Fig. 6: Core photos showing conglomerate facies (a) erosional lower contact in contact with the massive sandstone facies and slightly coarsening upward trend to the top (from core 6611/09-U-01, depth interval 322 m – 322 m), (b) upper contact of the conglomerate facies fining upwards into massive sandstone (from core 6611/09-U-01, depth interval 200 m – 201 m). The depth intervals are measure from top downward for each 1 metre long core, measurement on the side of the photos indicate 10 cm intervals downward (1 – 100 cm).

Massive sandstone facies

Description

The massive sandstone facies consists of light grey sandstone that lacks any bedding or sedimentary structures. Mud clasts can be found randomly dispersed throughout the facies. The mud clasts are angular and elongate (1 cm -> 5cm), or they can be small streaks (<1 cm) often aligned parallel to the bedding This poorly sorted facies has sub-angular grains, typically ranging from medium to very coarse sand. The thickness of this facies ranges from 20 to 70 cm. The lower contact tends to be sharp or erosional with underlying mudstone. Occasionally, the lower contact can be gradual from the conglomerate facies. Load and flame structures are also common (Fig. 7a) when the lower contact is with mudstone. The upper contact is mostly gradual into fining upward sandstone (Fig. 7b) or sandstone with traction structures (e.g. ripples). A sharp upper contact can also be seen with overlying chaotic facies.

Interpretation

This facies is very common throughout the cores. Massive sandstone is commonly associated with turbidity currents whose main grain support mechanism is turbulence. The massive fabric is the result of very rapid deposition or dumping of the coarser portion in a decelerating turbidity current (Lowe, 1982; Kneller & McCaffrey, 2003). As the flow decelerates so does the flow capacity, i.e. the ability to suspend sediment (Hiscott, 1994[a]). The rapid sediment fallout prevents the formation of any structures such as ripples, even though the grains may have been transported near the bed. Massive sandstone can also be deposited as under a quasi-steady, depletive high-density turbidity current where grain-by-grain deposition takes place due to hindered settling (Kneller & Branney, 1995). Load casts are very common because the density of the sand is higher than the underlying mud which has not been compacted yet at that time.

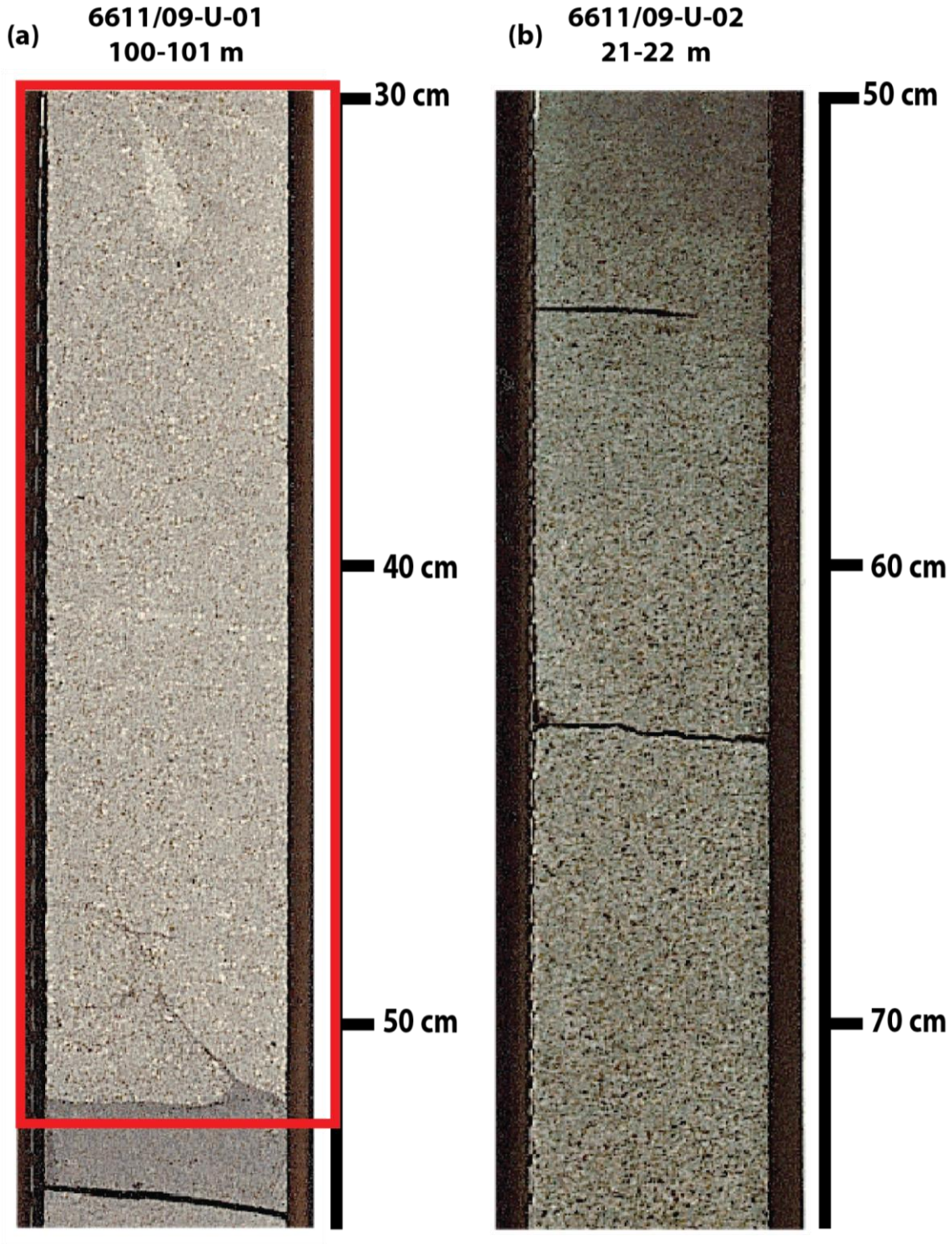

Fig. 7: Core photos showing massive sandstone facies, (a) lower contact with load and flame structures into mudstone (from core 6611/09-U-01, depth interval 100 m – 101 m), (b) interval of thick massive sandstone bed showing a gradual upper contact with fining upward sandstone (from core 6611/09-U-02, depth interval 22 m – 23 m). The depth intervals are measure from top downward for each 1 metre long core, measurement on the side of the photos indicate 10 cm intervals downward (1 – 100 cm).

Patchy sandstone facies

Description

The patchy sandstone facies is similar to the massive sandstone, but less homogenous in terms of grain size distribution. The sandstone consists of randomly distributed clusters or pockets with varying grain size. Fig. 8 shows the typical appearance of this facies, where there are patches of medium grained sandstone isolated within the very coarse, massive sandstone. The patches vary in size and shape. Occasionally, the patches are less obvious (Fig. 8a). The thickness of this facies is commonly 10 to 40 cm. There are few to no mud clasts present. Both upper and lower contacts (Fig. 8b) are mostly sharp with massive sandstone. In other cases, the contacts are sharp with chaotic or distorted heterolithic facies.

Interpretation

The isolated pockets of sand are interpreted to be the remnants of the parent flow that has not been fully mixed. This facies differ from division H3 in Haughton et al. (2009) that contains syn-depositional sand patches or injectites sourced from the lowest clean sandstone division (H1). The sand patches in H3 is similar to the sand injectite shown in Fig. 28. The sand patches found in this facies are not sand injectites because the contact with the host bed (in this case coarse sandstone) is not discordant. The grains within the patches does not have preferred orientation, such as shown within the sand injectite where the grains are aligned parallel to the discordant contact, which is very typical of sand injectites as they are intrusive (Hurst et al., 2011). The interpreted depositional mechanism of the patchy sandstone facies is by rapid deposition like the massive sandstone, but with the inclusion of different sand patches. This facies may be part of the late stage debris flow undergoing dilution into a high-density turbidity current.

.

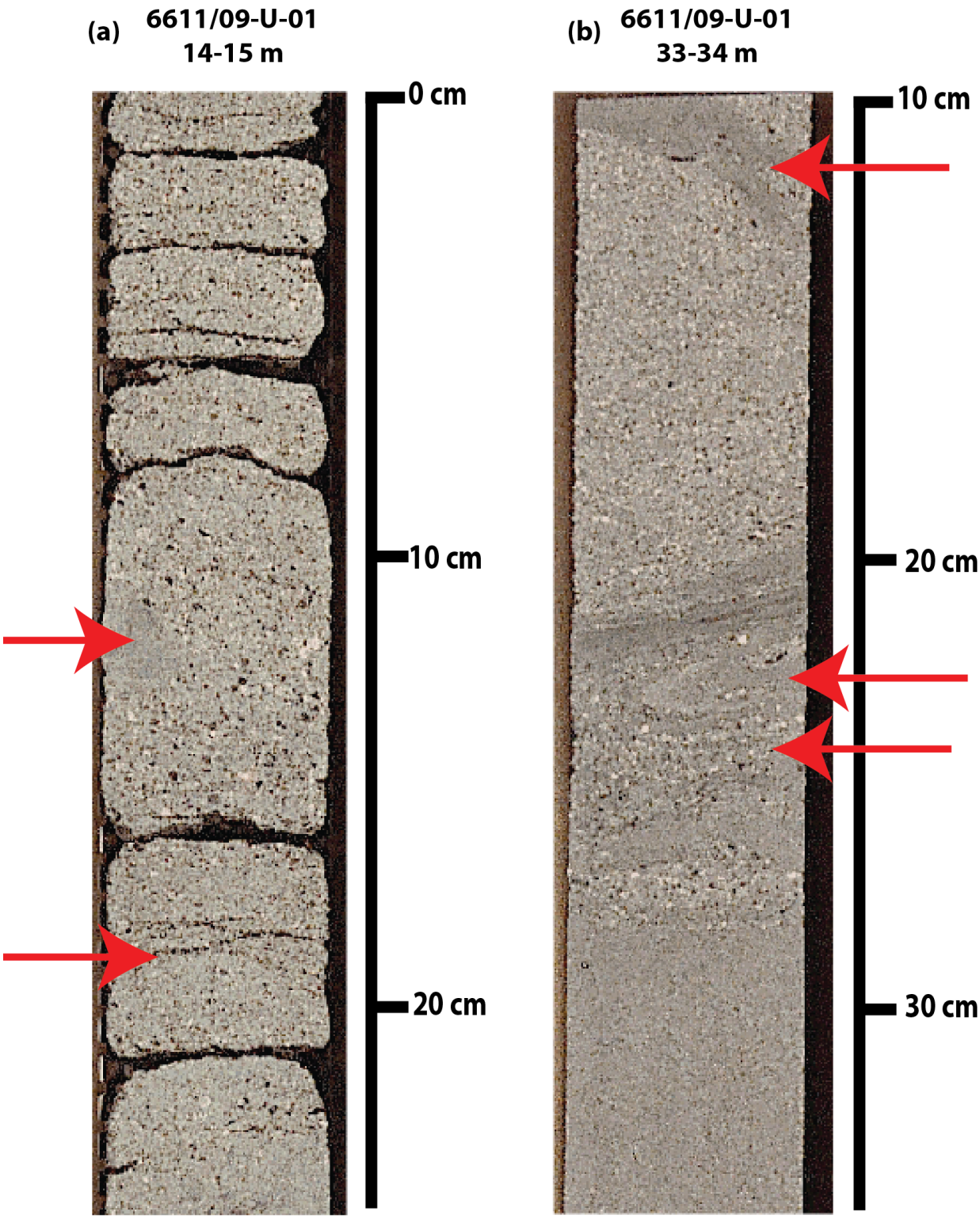

Fig. 8: Core photos showing patchy sandstone facies, (a) rounded pockets of fine sand within very coarse, massive-sandstone (from core 6611/09-U-01, depth interval 14 m – 15 m), (b) elongated and distorted sand patches with varying grain sizes within very coarse, massive sandstone (from core 6611/09-U-01, depth interval 33 m – 34 m). Red arrows point to the sand patches. The depth intervals are measure from top downward for each 1 metre long core, measurement on the side of the photos indicate 10 cm intervals downward (1 – 100 cm).

Coarsening upward sandstone facies

Description

The coarsening upward sandstone facies comprises of light grey sandstone that is inversely graded from the base upwards. The grains are angular with size ranging from fine to very coarse sand. The thickness of this facies is bimodal: either as very thin beds (1 – 3 cm) or medium beds (10 – 30 cm). This facies commonly lacks any sedimentary structures, nor does it contain mud clasts. The lower contact tends to be sharp such as in Fig. 9b with planar laminated sandstone below this facies. In other cases, the lower contact is gradual from underlying massive sandstone, such as in Fig. 9a where the largest grains are scattered and there is no visible bed boundary. The upper contact is mostly gradual into massive sandstone or conglomerate facies.

Interpretation

Similar to the conglomerate facies, inverse grading can be the result of grain to grain collision and intergranular shear which forces the coarser grain upwards and filters the finer grains towards the base of the flow. In this case the support mechanism is dispersive pressure and the sediment deposits through frictional freezing. This would be the possible explanation of the thin coarsening upwards sandstone at the base of massive sandstone. This facies is often associated with a grain flow or a high-density turbidity current. Another explanation to how inverse grading can form is caused by lateral variation in a turbidity current, where most of the coarse grains concentrated near the base of the flow separate completely from the body and form coarse tail grading (Hand, 1997), where the slower basal layer deposits on top of the sand that the head deposited first.

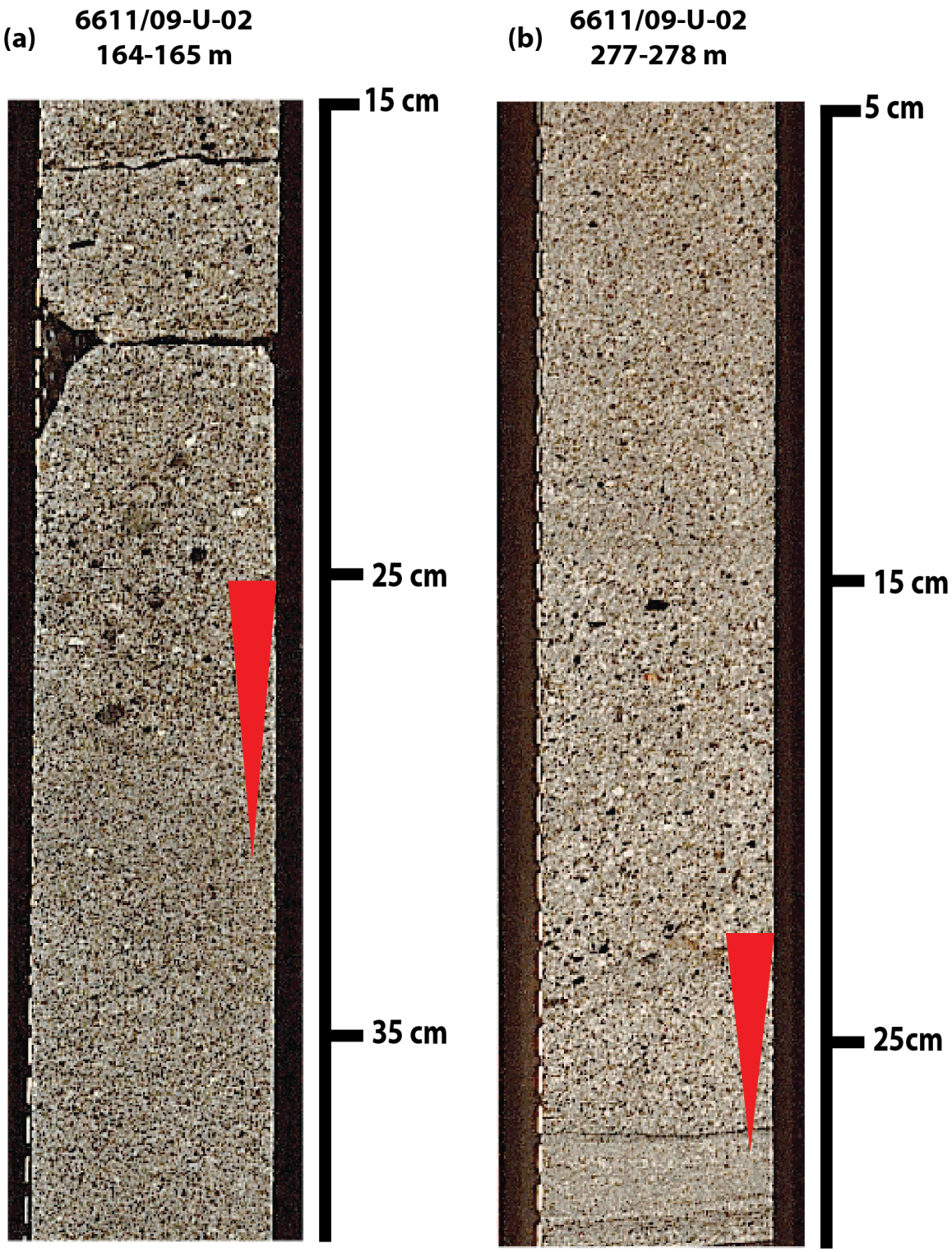

Fig. 9: Core photos showing coarsening upward sandstone facies that transition to fining upward facies, (a) gradual coarsening up from massive sandstone (from core 6611/09-U-02, depth interval 164 m – 165 m), (b) thin coarsening upward bed at the base of a turbidite (from core 6611/09-U-02 depth interval 277 m – 278 m). The depth intervals are measure from top downward for each 1 metre long core, measurement on the side of the photos indicate 10 cm intervals downward (1 – 100 cm).

Fining upward sandstone facies

Description

The fining upward sandstone facies comprises of light grey sandstone that is normally graded from the base upwards. The grains typically range from fine to coarse sand, and are sub-rounded. The thickness of this facies has a wide range from 5 – 50 cm thick. The lower contact is mostly gradual from massive sandstone, such as in Fig. 10. In other cases the lower contact is sharp and shows erosion of underlying mudstone. The upper contact is gradational into sandstone with traction structures, i.e. planar laminated (Fig. 10) or rippled sandstone.

Interpretation

This facies is deposited by a turbidity current as it is the result of aggradational deposition. Normal grading is a common feature of an unsteady flow, where the grains supported by turbulence undergo grain-by-grain deposition as the turbidity current decelerates. When the flow decelerates, so does the flow strength which means the ability to carry grains decreases. In result, the turbidity current progressively deposits smaller grains. Fining upward sandstone can be found in both low- and high-density turbidity currents.

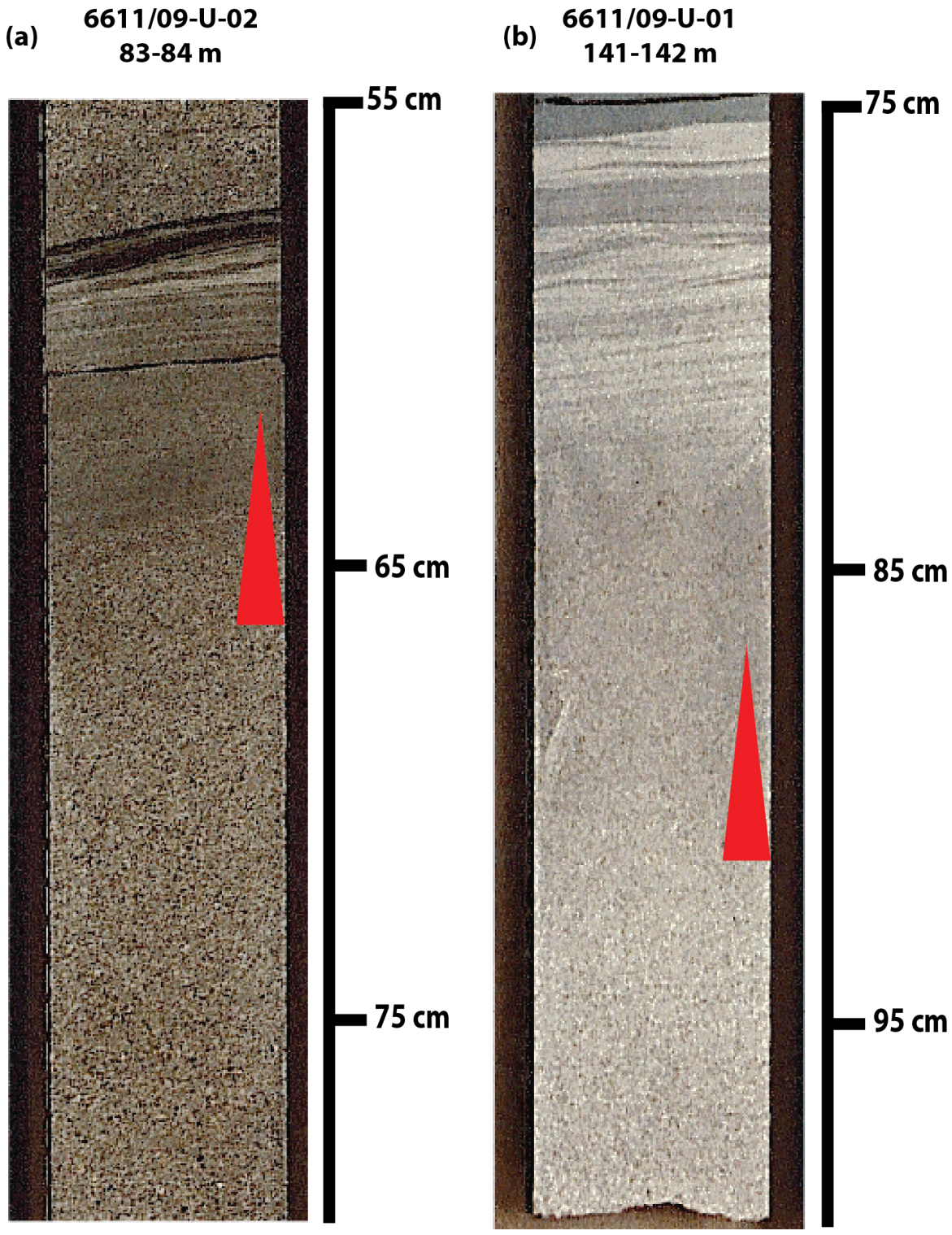

Fig. 10: Core photos showing fining upward sandstone facies in a turbidite facies association, (a) fining upwards into parallel laminated sandstone (from core 6611/09-U-02, depth interval 83 m – 84 m), (b) fining upwards sandstone with Bouma B, C and E (from core 6611/09-U-01, depth interval 141 m – 142 m). The depth intervals are measure from top downward for each 1 metre long core, measurement on the side of the photos indicate 10 cm intervals downward (1 – 100 cm).

Parallel-laminated sandstone facies

Description

The parallel laminated sandstone facies comprises of light- to medium grey sand beds that show planar, parallel stratification of less than a centimetre thick. Occasionally, this facies shows an overall fining upward trend. The grains range from fine to medium sand. Each lamina is about 1 cm or less, the thickness of this facies is typically about 5 – 30 cm thick in total. The thin bedded parallel-laminated sandstone often caps the chaotic facies, whilst the thicker, parallel-laminated sandstone occurs together with fining upwards sandstone. Occasionally, thin mud streaks of about 0.2-0.5 cm are observed parallel to the laminae. The lower contact shows a gradual change from a massive sandstone such as in Fig. 11a, or from a fining upward sandstone. In other cases, the lower contact is sharp and erosive such as in Fig. 11b. The upper contact is gradual into rippled sandstone or massive mudstone.

Interpretation

This facies is commonly associated with a low-density turbidity current that deposits Bouma T_b and T_d. Parallel laminated sandstone formed beneath upper stage plane bed (Collinson et al., 2006).

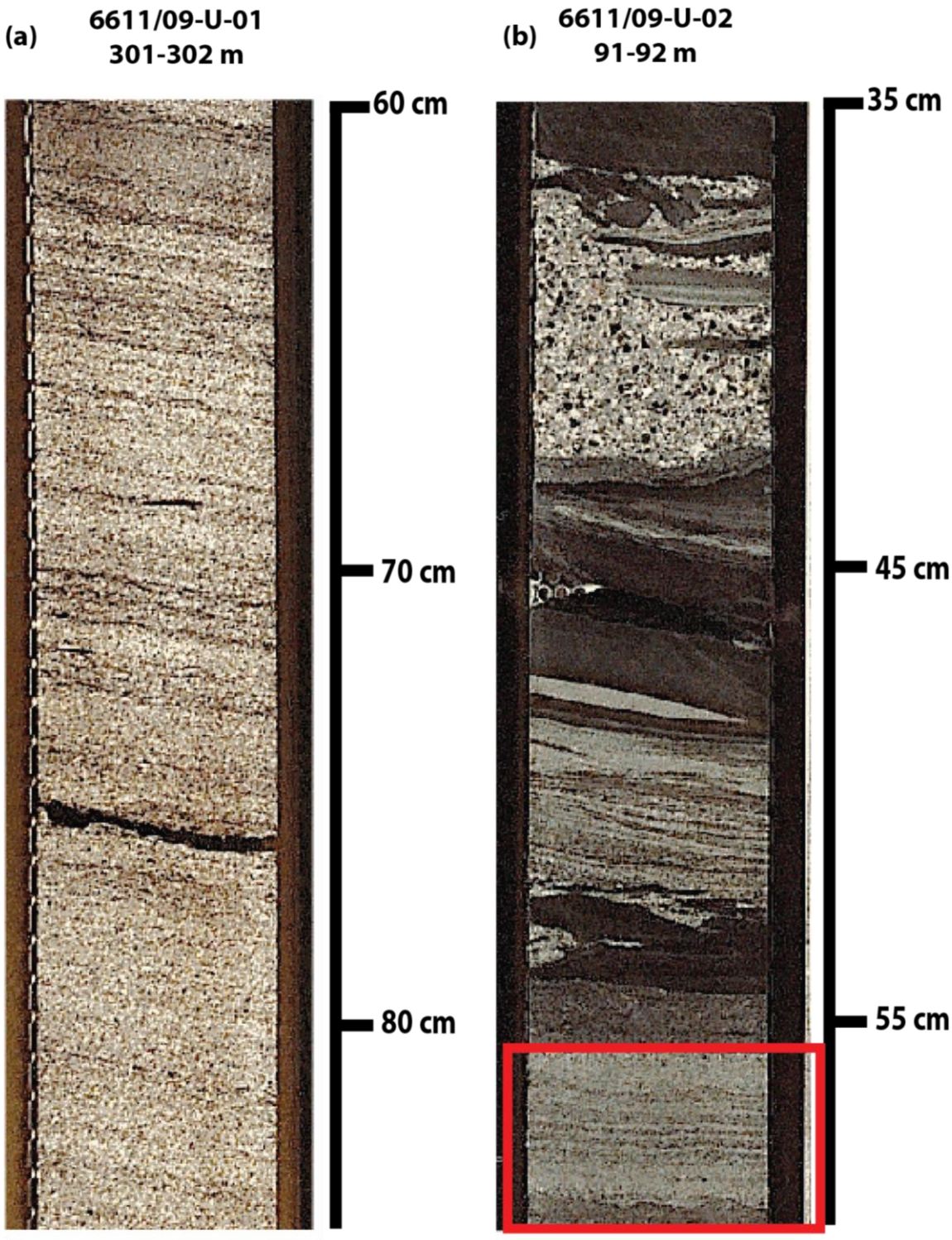

Fig. 11: Core photos showing two types of planar laminated sandstone, (a) thick bed (>30 cm) showing planar-laminated sandstone (from core 6611/09-U-01, depth interval 301 m – 302 m), (b) red box showing thin (<10cm) planar-laminated sandstone with erosive base (from core 6611/09-U-02, depth interval 91 m – 92 m). The depth intervals are measure from top downward for each 1 metre long core, measurement on the side of the photos indicate 10 cm intervals downward (1 – 100 cm).

Distorted heterolithic facies

Description

This facies consists of interbedded mudstone and sandstone, which has been sheared and deformed, often with sharp and serrated edges. The original lamination is still visible. This facies varies in grain composition, but the common grain sizes are clay, and silt or fine sand. This facies is discordant with the adjacent beds. The thickness of this facies range from 10 to 20 cm. Both upper and lower contact are sharp with the adjacent beds such as in Fig. 12a, or it can be encased in a massive sandstone such as in Fig. 12b. The upper contact with the overlying very coarse sandstone in Fig. 12b is sharp.

Interpretation

This facies reflects the original structure of previous beds that have either been eroded or disturbed, generating a slump as a result. The slump is indicated by the sheared layers which have not been broken up yet. This indicate that this facies was transported in a dense flow. Thin bedded, distorted heterolithic beds tend to show original layering which indicate a slump type. In this case, the deposition mechanism would be through en masse freezing.

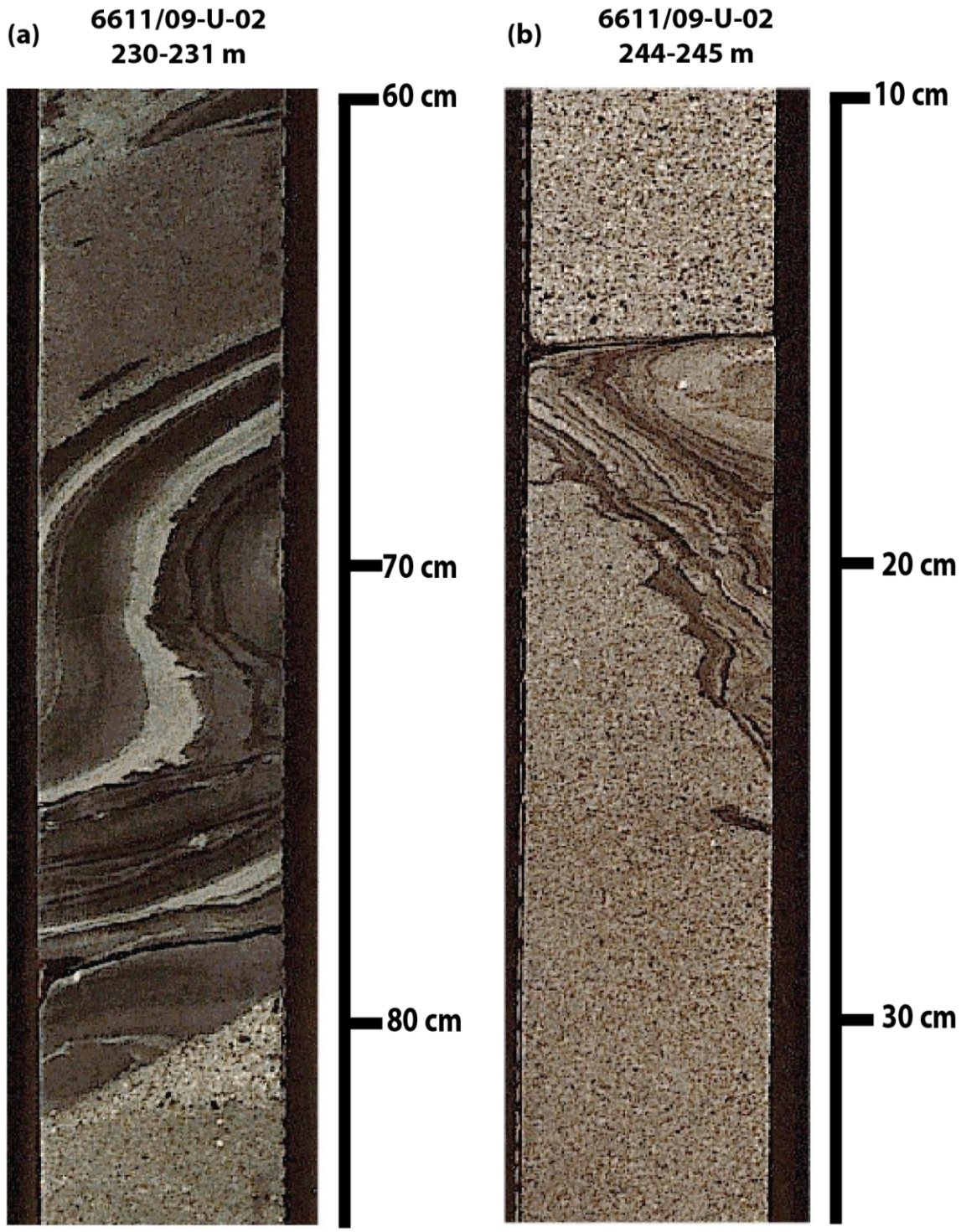

Fig. 12: Core photos showing different variation of distorted heterolithic beds, (a) muddy distorted beds with sharp lower and gradual upper contact into chaotic sandstone facies (from core 6611/09-U-02, depth interval 230 m -231 m), (b) sandy distorted bed encased in a massive sandstone with sharp upper and lower contacts (from core 6611/09-U-02, depth interval 244 m -245 m). The depth intervals are measure from top downward for each 1 metre long core, measurement on the side of the photos indicate 10 cm intervals downward (1 – 100 cm).

Chaotic facies

Description

This facies consists of muddy sandstone or clean sandstone that gradually changes into muddy sandstone, with abundant mud clasts present at the top. The mud clasts are very angular, vary in size from less than 1 cm to >5cm, float within the muddy sandstone, and often laminated (Fig. 13). The laminated clasts are often sheared such as in Fig. 13a in the top left corner, or they still have the original lamination preserved such as in Fig. 13b. This facies often have sand patches as well (1 – 4 cm). The thickness of this facies ranges from 10 to 20 cm. The lower contact, when mudstone underlies this facies, is mostly sharp. Occasionally, when underlain by muddy sandstone facies, the lower contact can be gradual. The upper contact is sharp with an overlying massive sandstone or a mudstone, or gradual with overlying thin sand interbedded mudstone.

Interpretation

This facies is a typical characteristic of a debris flow where the sediment is supported by matrix strength. The floating mud clasts and sand patches are suspended within the cohesive muddy sandstone that provide support. The sediment is deposited by cohesive freezing.

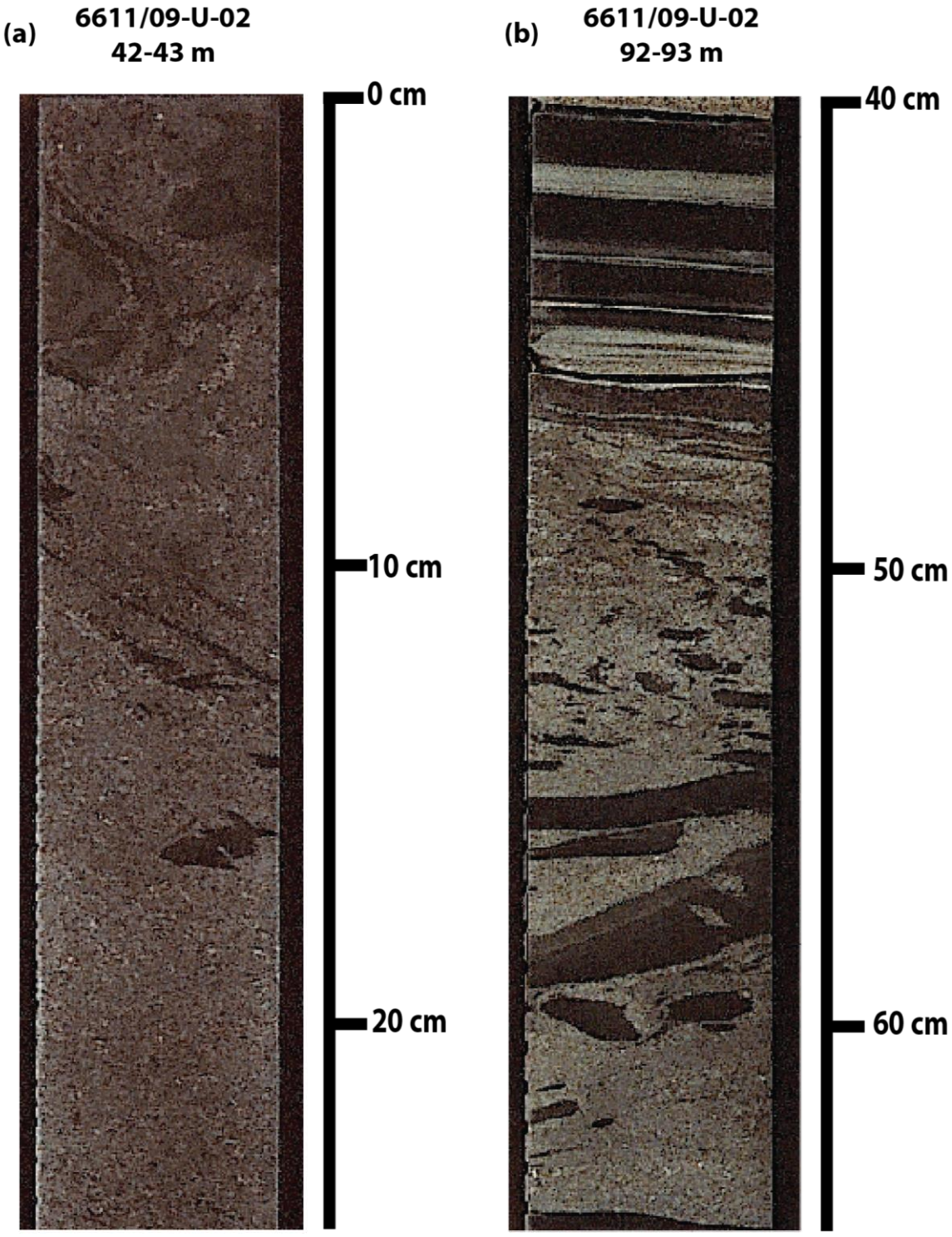

Fig. 13: Core photos showing chaotic facies with floating mud clasts, (a) gradual lower contact from muddy sandstone into chaotic facies with the randomly oriented mud clasts (from core 6611/09-U-02, depth interval 42 m -43 m), (b) slightly oriented clasts with the bigger clasts near to the base of the bed (from core 6611/09-U-02, depth interval 92 m -93 m). The depth intervals are measure from top downward for each 1 metre long core, measurement on the side of the photos indicate 10 cm intervals downward (1 – 100 cm).

Ripple sandstone facies

Description

The ripple sandstone facies comprises of light grey, very thin beds with ripples. The grains are subrounded with grain size ranges from fine to medium sand. The thickness of this facies ranges from 1 – 5 cm. Occasionally, the individual foresets are not so clear but the lenticular shape of this facies helps the identification as ripples. The ripples often have mud streaks which cause this facies to appear heterolithic, such as in Fig. 14b (bottom arrow). The lower contact with underlying massive sandstone or parallel laminated sandstone tends to be sharp or gradual (Fig. 14). The upper contact is mostly sharp with overlying interbedded sandstone-mudstone facies or massive mudstone facies.

Interpretation

Ripples are formed by lower flow regime current that carries the sediment by bedload transport and deposits by traction sedimentation. This facies indicates a low-density turbidity current and is commonly known as Bouma $T_{c.}$

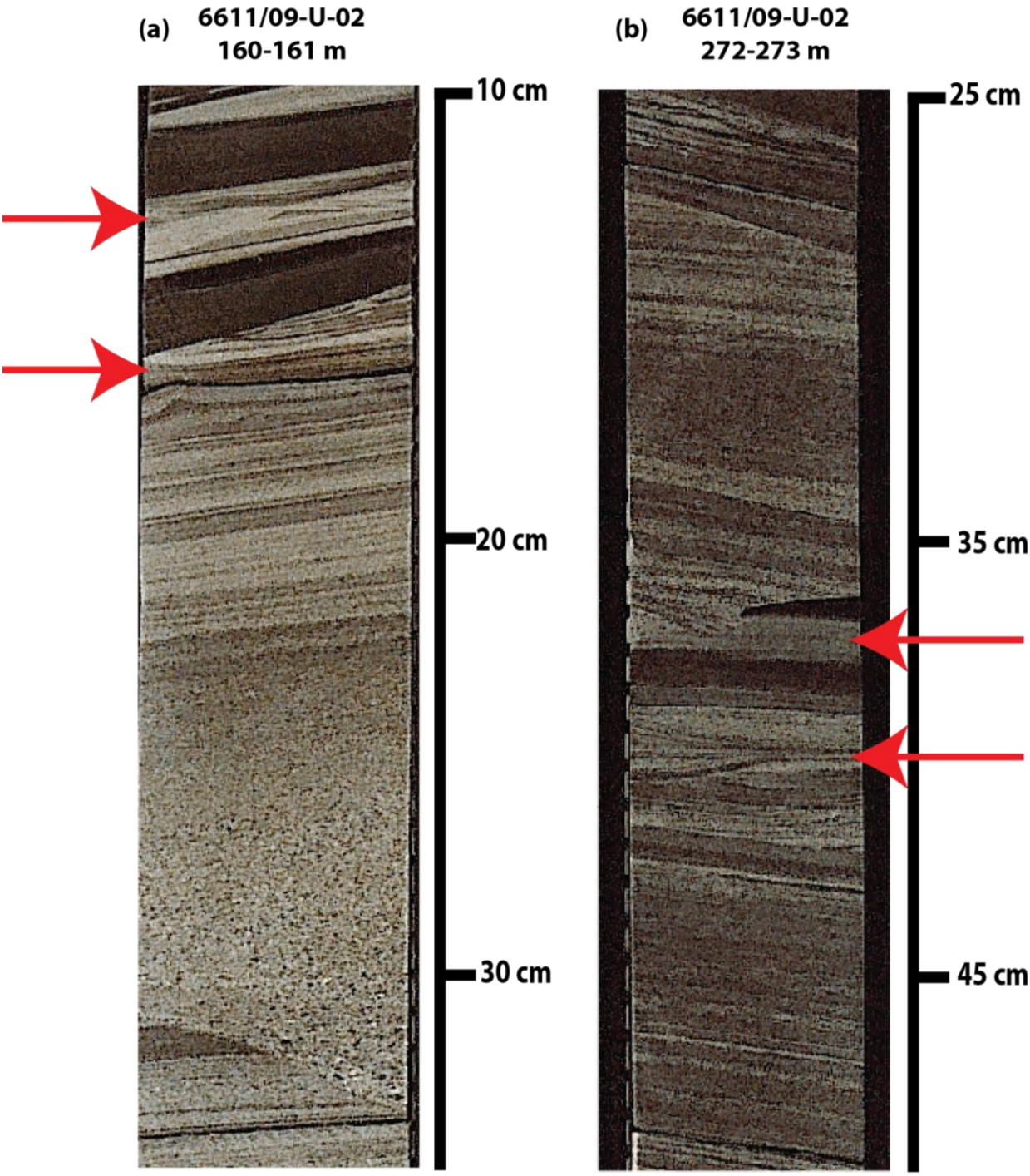

Fig. 14: Core photos of very thin ripple sandstone facies pointed at by the red arrows (a) ripples in a typical Bouma sequence (as Bouma T_c) with gradual lower contact with planar laminated sandstone (from core 6611/09-U-02, depth interval 160 m -161 m), (b) sequences of low density turbidites consisting of planar laminated sandstone, ripple sandstone, and massive mudstone (from core 6611/09-U-02, depth interval 272 m -273 m). The depth intervals are measure from top downward for each 1 metre long core, measurement on the side of the photos indicate 10 cm intervals downward (1 – 100 cm).

Thinly layered interbedded sandstone and mudstone

Description

This facies consists of alternating laminae of sandstone and mudstone. The sandstone is typically very fine to fine grained. The planar lamination can have sharp lower and upper contacts, but sometimes it can also be gradual as very thin fining upward laminae. This facies often occurs in thick sequences (30 – 50 cm) as shown in Fig. 15 and Fig. 16. Occasionally, the sandstone contains ripples (Fig. 15), where loading of the sand is common. The lower contact is mostly sharp with ripple sandstone facies. The upper contact is gradual into massive mudstone facies.

Interpretation

The thin alternating layers of sandstone and mudstone indicate multiple events of alternating current, where the sand is deposited by traction sedimentation overlain by suspension settling of the mud.

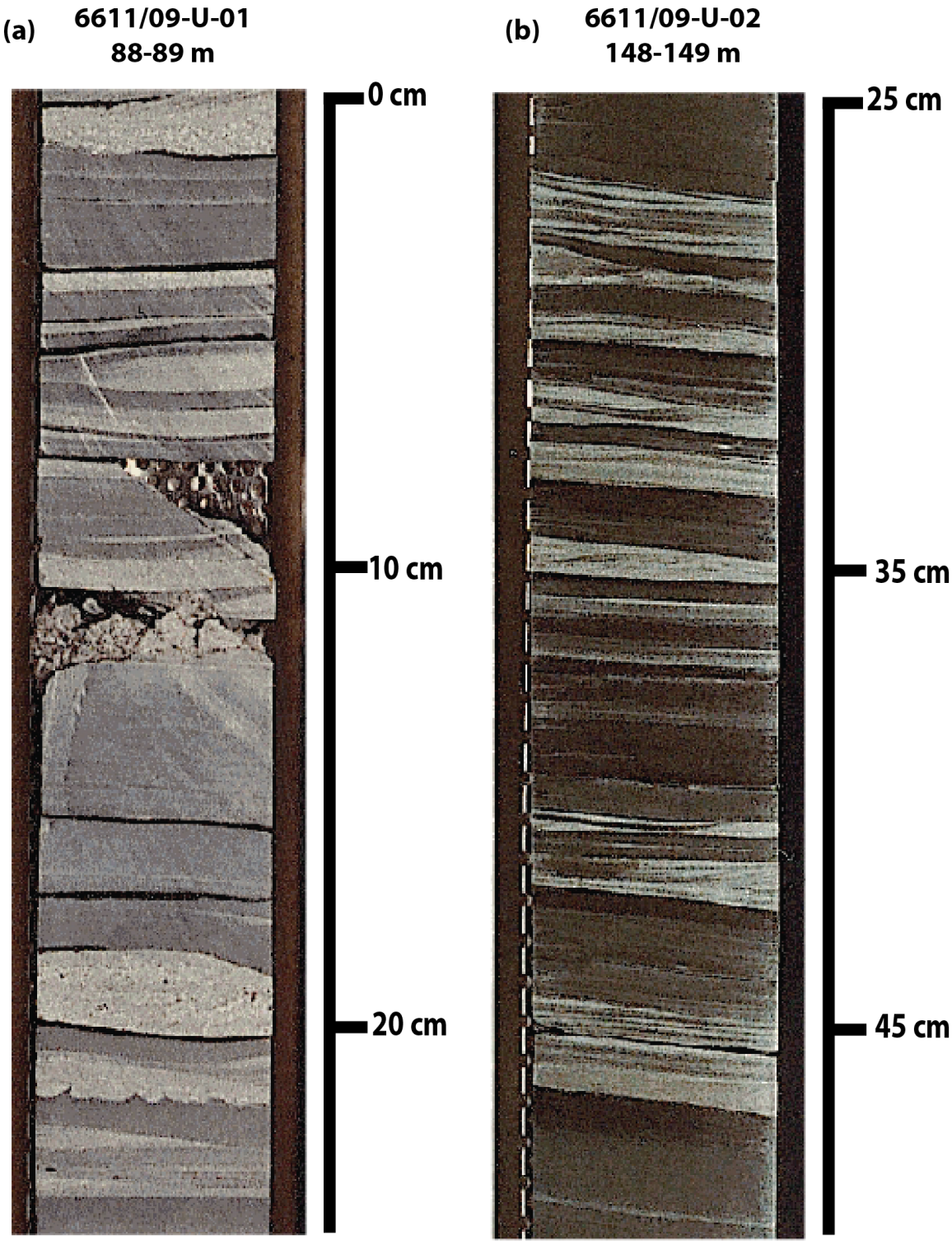

Fig. 15: Core photos showing loaded ripple, (a) very thin sandstone bed loading into the mud with vague ripple internal structures, thus they look like lenticular beds (from core 6611/09-U-01, depth interval 88 m -89 m), (b) very thin sandstone with clearer ripple structures, loading is more apparent at the upper part of this interval (from core 6611/09-U-02, depth interval 148 m -149 m). The depth intervals are measure from top downward for each 1 metre long core, measurement on the side of the photos indicate 10 cm intervals downward (1 – 100 cm).

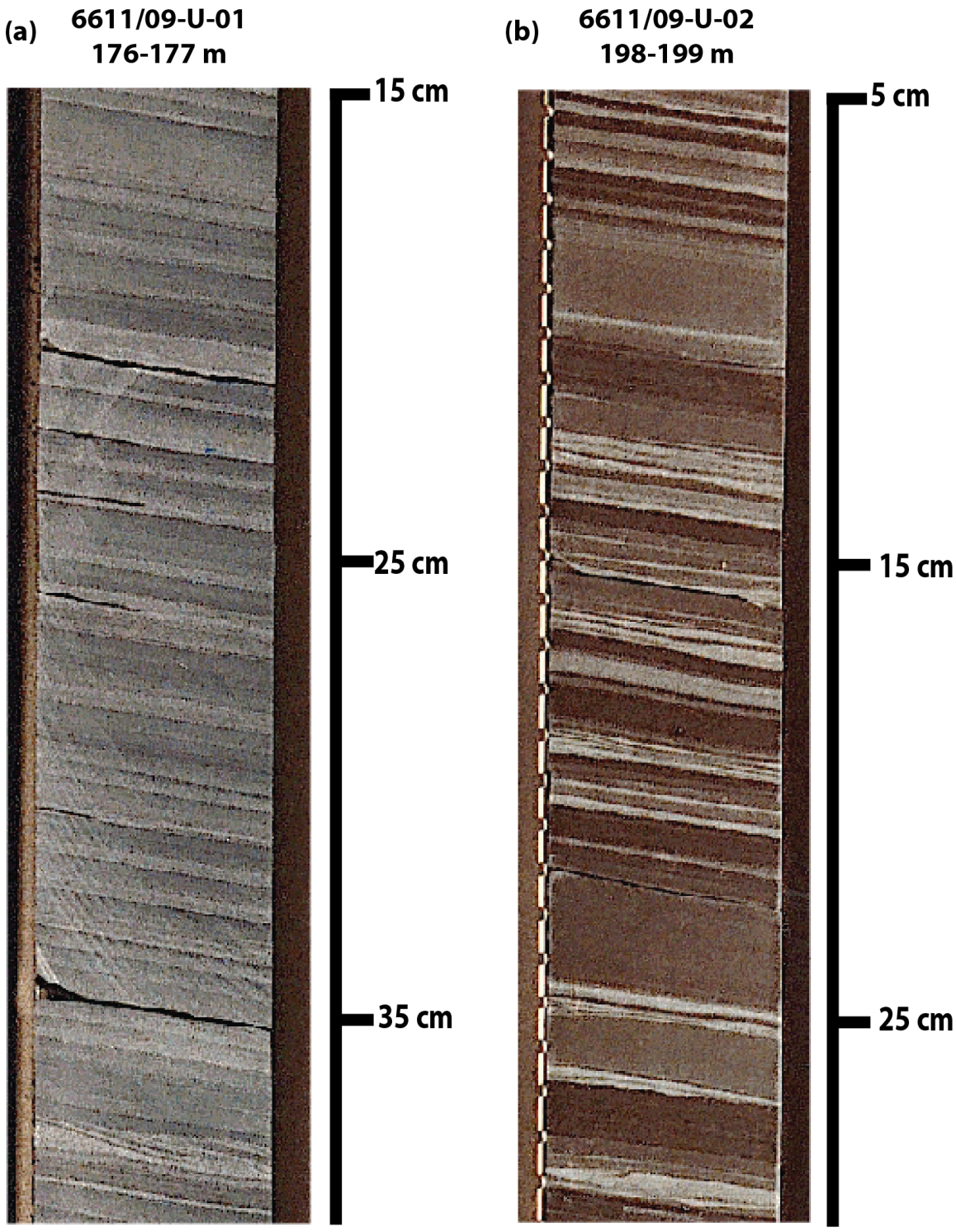

Fig. 16: Core photos showing the thinly layered interbedded sandstone and mudstone, (a) very thin layers of this facies with gradual contact and fining up sequences (from core 6611/09-U-01, depth interval 176 m - 177), (b) alternating mudstone-sandstone with sharp lower and upper contacts, the more wavy contact indicates loading or rippled structure (from core 6611/09-U-02, depth interval 198 m -199 m). The depth intervals are measure from top downward for each 1 metre long core, measurement on the side of the photos indicate 10 cm intervals downward (1 – 100 cm).

Muddy sandstone facies

Description

The muddy sandstone facies consists of structureless, dark grey, mud-rich sandstone with angular mud clasts up to 5 cm in size dispersed throughout the facies (Fig. 17). The sandstone is fine to coarse grained with angular sphericity. The thicknesses range from thin beds (less than 10 cm) to medium (~20 cm) beds. The lower contact is mostly sharp with massive sandstone. The upper contact is sharp and irregular with a mudstone facies. Occasionally, the upper contact is more gradual into a sand interbedded mudstone facies.

Interpretation

This facies is similar to the chaotic facies, but it is more homogenous and contains fewer mud clasts. The sediment is supported by the matrix strength and it deposited due to cohesive freezing.

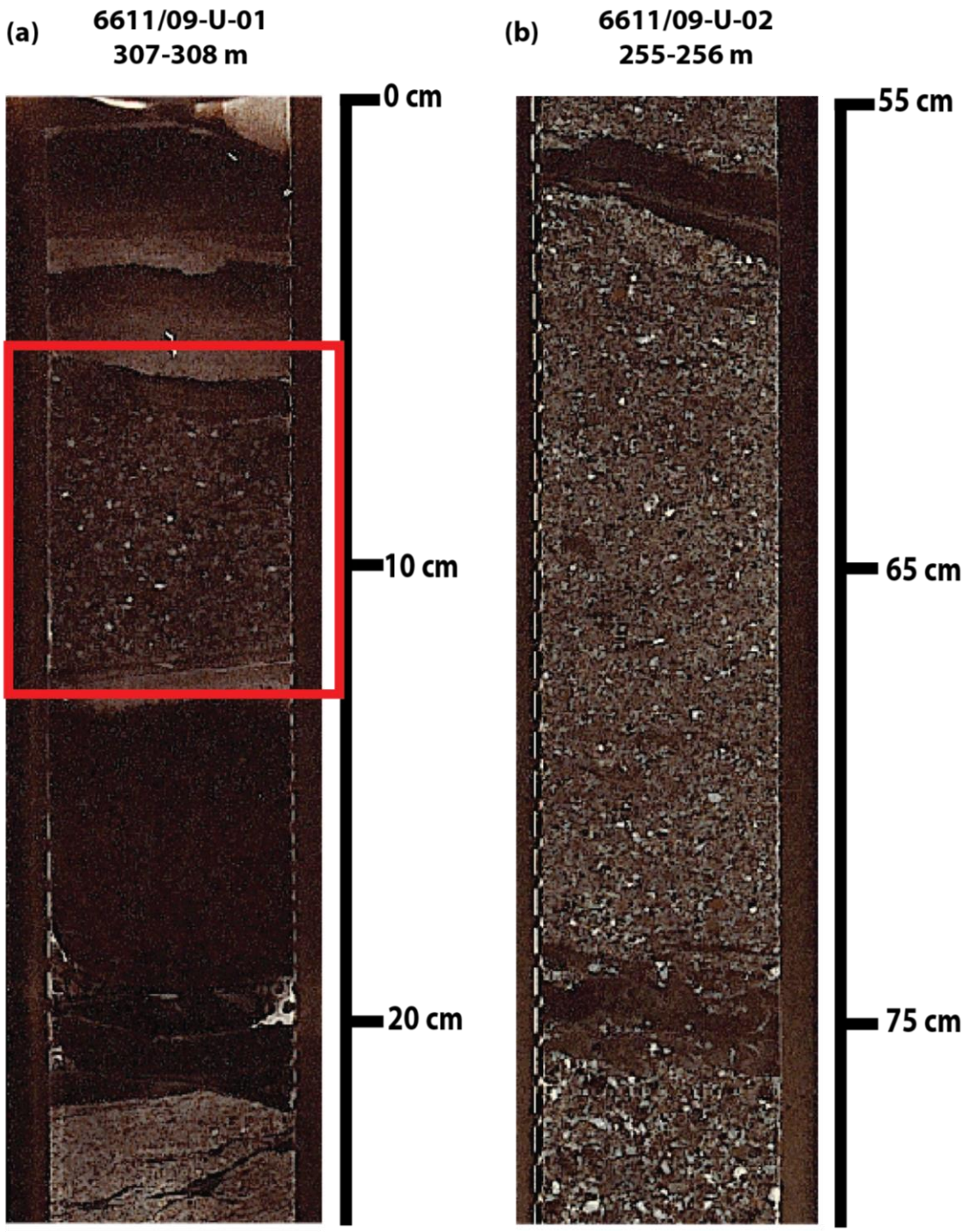

Fig. 17: Core photos showing muddy sandstone facies (a) thin bedded muddy sandstone (from core 6611/09-U-01, depth interval 307 m -308 m), (b) thick bedded muddy sandstone with large mud clasts (from core 6611/09-U-02, depth interval 255 m -256 m). The depth intervals are measure from top downward for each 1 metre long core, measurement on the side of the photos indicate 10 cm intervals downward (1 – 100 cm).

Sandy mudstone facies

Description

The sandy mudstone facies consists of dark grey mudstone with floating sand clasts or pebbles. This facies is generally structureless, but it often has silt lenses and rounded mud clasts (1 – 2 cm). The thickness of the sandy mudstone ranges from 5 – 12 cm. Fig. 18 shows the typical appearance of this facies, notice that there's no particular grading of the clasts within the mud in Fig. 18b. The lower contact is mostly sharp with massive mudstone facies. The upper contact tends to be gradual with muddy sandstone or sand interbedded mudstone.

Interpretation

This facies is a typical characteristic of a mud flow where the majority of the sediment is mud (silts and clays). The sediment is fully suspended in the muddy fluid and any coarse grain would be supported by the matrix strength. This laminar flow is deposited by cohesive freezing.

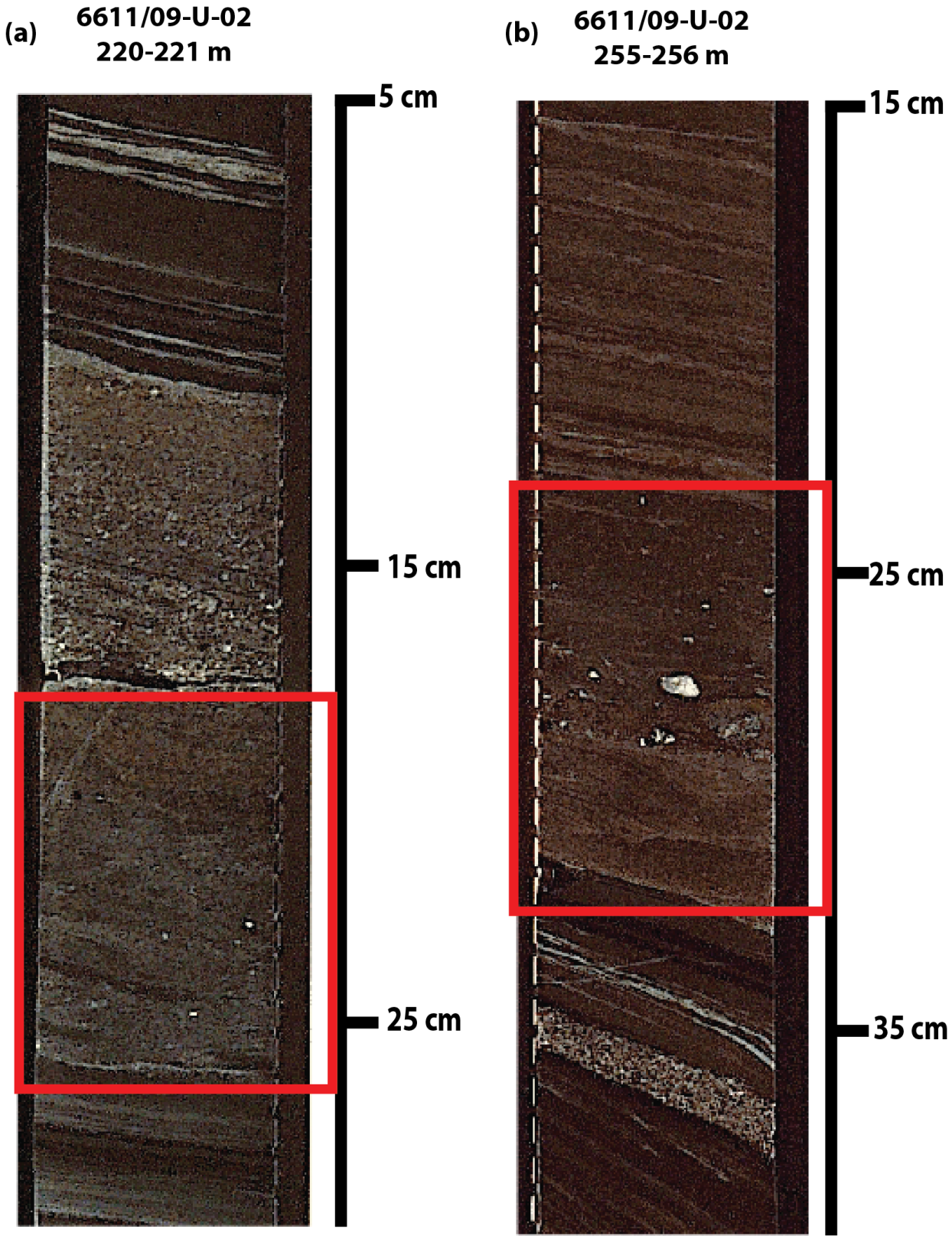

Fig. 18: Core photos showing sandy mudstone facies with floating sand grains and pebbles (a) from core 6611/09-U-02, depth interval 220 m - 221 m, (b) from core 6611/09-U-02, depth interval 255 m -256 m. The depth intervals are measure from top downward for each 1 metre long core, measurement on the side of the photos indicate 10 cm intervals downward (1 – 100 cm).

Laminated mudstone facies

Description

The laminated mudstone facies consists of mudstone with medium and dark grey mud laminae (Fig. 19). The thickness of this facies range from very thing (1 – 3 cm) to thin (<10 cm). The planar lamination is often unclear because the colours are not contrasting. On closer inspection by using the thin sections (Section 3.2), the laminated mudstone contains ripples and sometimes interbedded ripple and massive mudstone. The lower contact is mostly sharp with ripple sandstone or sand interbedded mudstone facies. The upper contact is gradual into massive mudstone facies, or sharp with sand interbedded mudstone (often with small loading).

Interpretation

Refer to Section 3.2

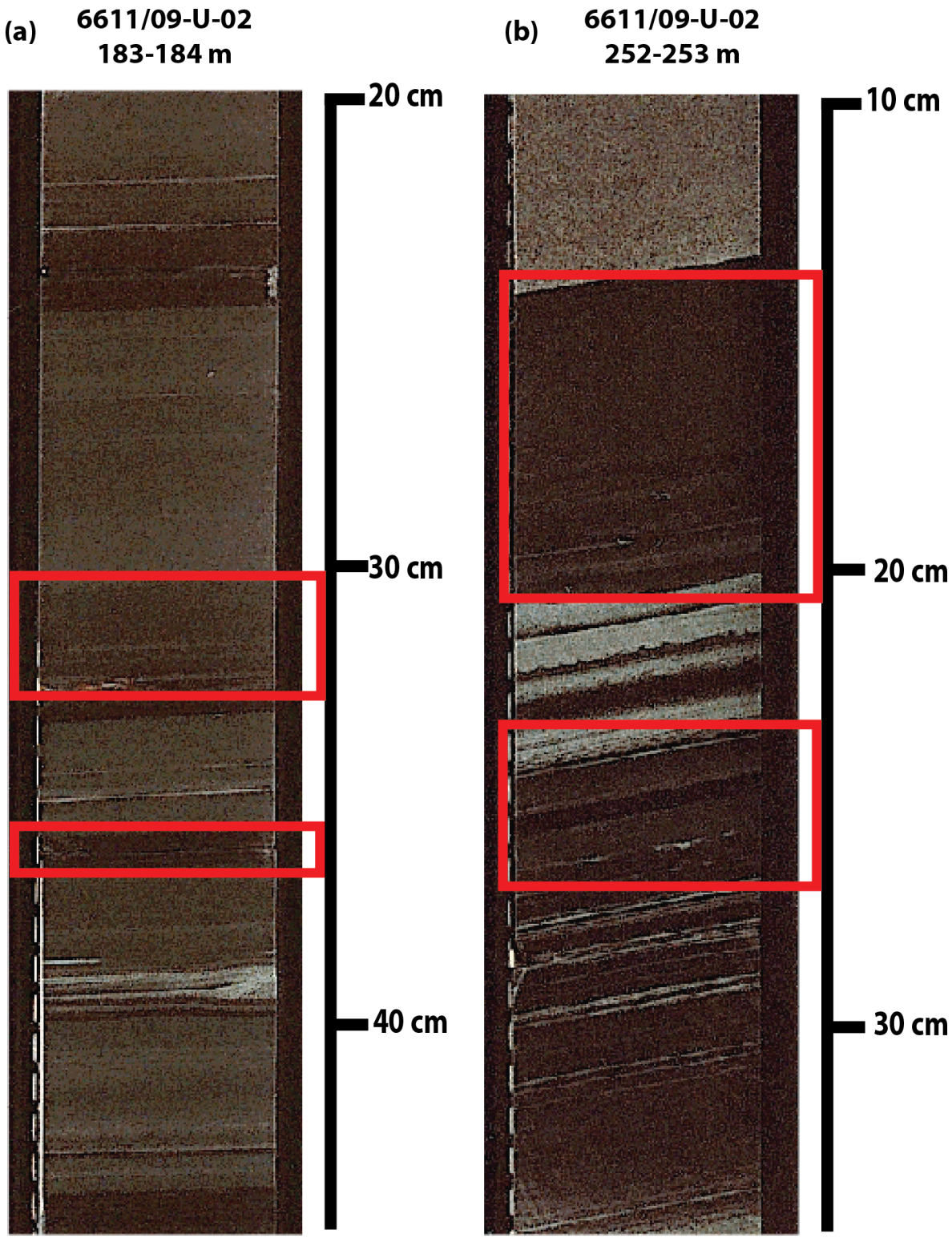

Fig. 19: Core photos showing laminated mudstone (a) from core 6611/09-U-02, depth interval 183 m - 184 m, (b) from core 6611/09-U-02, depth interval 252 m -253 m. The depth intervals are measure from top downward for each 1 metre long core, measurement on the side of the photos indicate 10 cm intervals downward (1 – 100 cm).

Massive mudstone facies

Description

This facies comprise of dark grey, massive mudstone (Fig. 20). The thickness of this facies ranges from 3 - 40 cm. On closer inspection by using the thin sections (Section 3.2), the massive mudstone appears to be inhomogeneous, with discontinuous layers of silt and what appears to be mud clasts. The lower contact is sharp with sand interbedded mudstone or ripple sandstone. The upper contact is sharp with massive sandstone and often have loading or erosional structures.

Interpretation

Refer to Section 3.2.

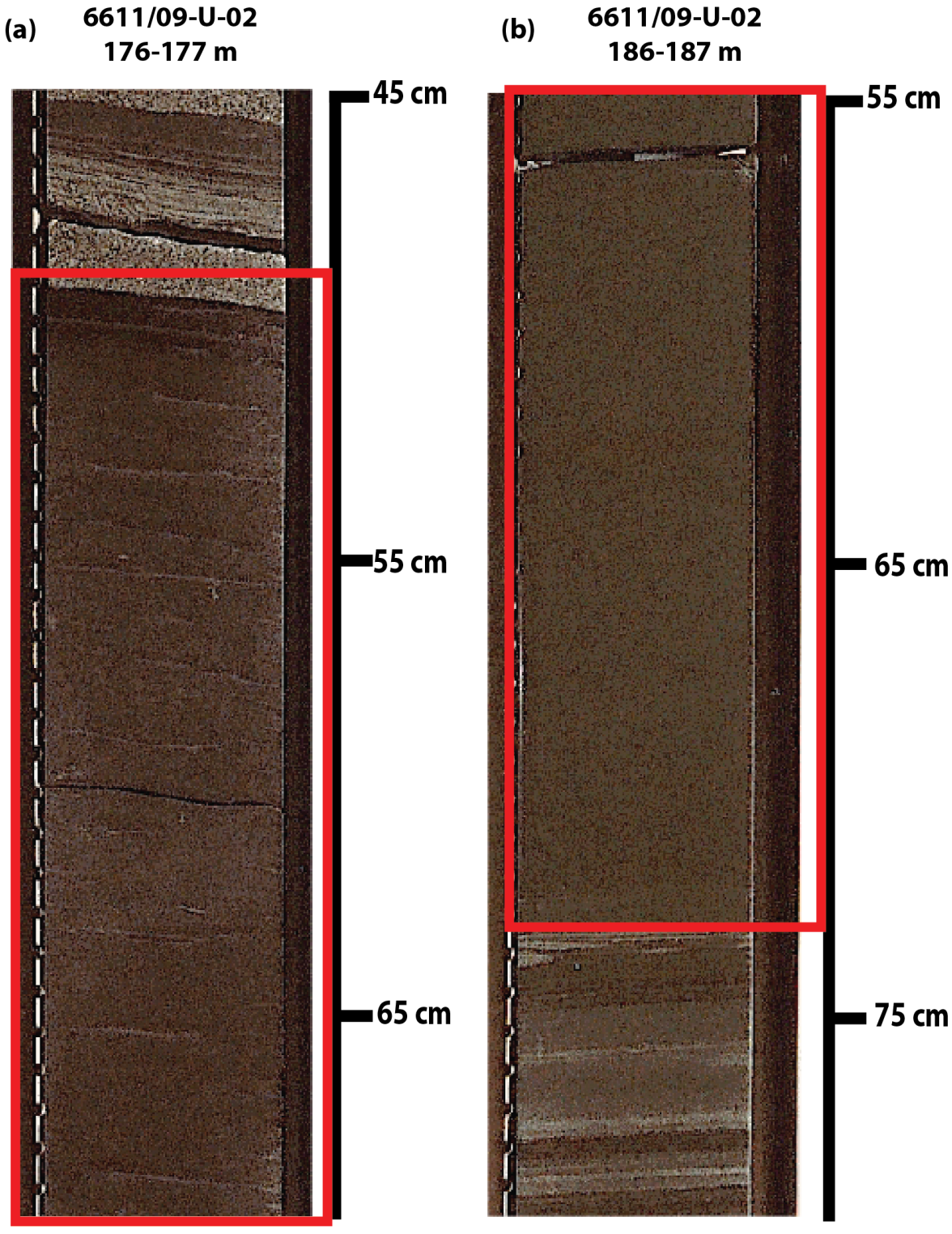

Fig. 20: Core photos showing massive mudstone, (a) upper contact is sharp, often preserved loading and flame structure or erosional contact (from core 6611/09-U-02, depth interval 176 m – 177 m), (b) gradual lower contact with laminated mudstone, with few blobs of very thin sandstone encased in the mud, possibly from loading (from core 6611/09-U-02, depth interval 186 m – 187 m). The depth intervals are measure from top downward for each 1 metre long core, measurement on the side of the photos indicate 10 cm intervals downward (1 – 100 cm).

3.2 MICROSTRUCTURES IN MUDSTONE

Seven thin sections, 4 from laminated mudstone facies and 3 from massive mudstone facies, were observed to have microstructures including ripples, planar laminations, normal grading and inhomogeneous fabric.

Description

Two of the laminated mudstones contain coarse, discontinuous, lenticular silt layers that are interspersed with fine material (Fig. 21 and Fig. 22). The silt layers taper laterally where dark, fine (clay) layers are present above and below the silt layers. The lenticular silt layers resemble downcurrent dipping ripple foresets, whilst the dark clay layers may be the result of compaction of clay clast deposit, which form thin sheets (similar to fig. 11B in Schieber et al., 2010). In the thin section shown in Fig. 21, these ripples and clay sheets were observed to occur throughout the whole thin section, whilst in the thin section shown in Fig. 22, the ripple and clay sheet layers are thinner, and interlaminated with massive mudstone.

Interpretation

Muds have been found to form migrating ripples that are generated by floccules (Schieber et al., 2007). Since floccules are bigger than individual mud grains, they can be transferred to the bedload and form structures just like sand grains. The ripples in Fig. 21 and Fig. 22 are similar to the barchan shaped silt ripples found in an experiment by Yawar & Schieber (2017), where coarse silt grains (30 – 60 μm) segregate from the mud and form ripples. In their experiment, it was observed that the silt grains were first incorporated into the floccules and get transported on to the bed. Later, the floccules break apart, releasing the silt grains due to the inertial forces of the quartz which later form the silt ripples, both the silt and the clay floccules can form separate migrating ripples. The critical velocity for clay floccule sedimentation was concluded to be approximately at 25 cm/s (Schieber et al., 2007; Yawar & Schieber, 2017). The dark layers could indicate the product of rip up mud clasts that were originally water-rich and have been compacted into thin sheet-like appearance (Schieber et al., 2010).

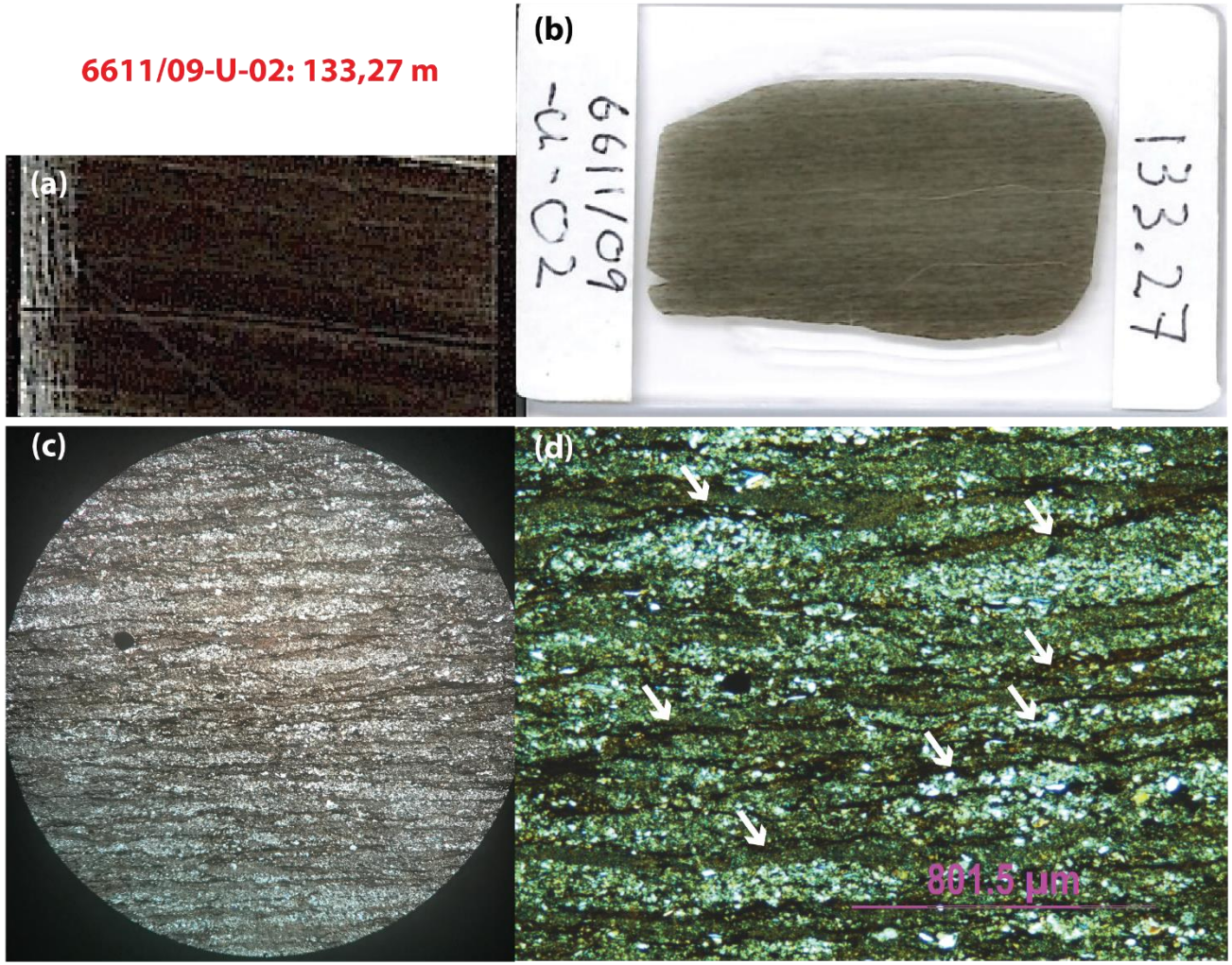

Fig. 21: Laminated mudstone that shows silt ripples (a) core photo of the dark grey laminated mudstone (depth interval 133.27 m – 133.32 m), (b) full thin section scan, (c) with magnification of 5x , field of view is 3.6 mm, (d) discontinuous, lenticular silt layers pointed at by the arrows.

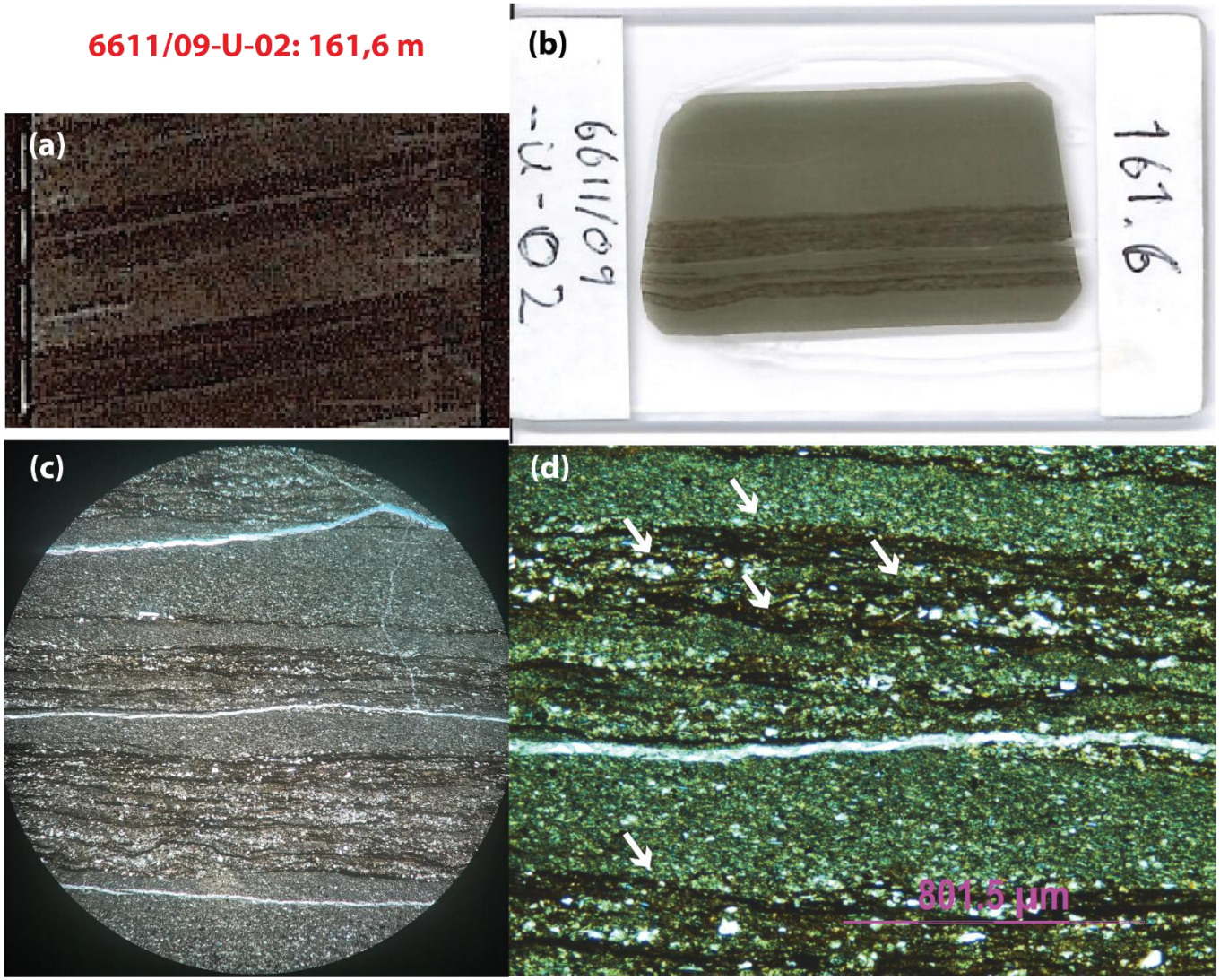

Fig. 22: Laminated mudstone that shows silt ripples, interlaminated with massive sandstone (a) core photo of the section (depth interval 161.6 m – 161.65 m), (b) full thin section scan, (c) with magnification of 5x, field of view = 3.6 mm, (d) discontinuous, lenticular silt layers pointed at by the arrows.

Description

Another laminated mudstone facies shown in Fig. 23, does not contain ripples. The laminated mudstone was observed to contain interlaminated massive mudstone and calcareous fossil rich layers. The massive mudstone contains both silt- and clay-sized particles and appears homogenous, whilst the fossil rich layers are mixed with quartz sand. The fossils contained in the fossil rich layers are mostly broken up, although some were recognized to be ooids, shell fragments (shown by white arrows in Fig. 23c-d) and foraminifera.

The last laminated mudstone type, shown in Fig. 24 consists of plane-parallel laminae composed of interlaminated silt layers and fine silt and clay layers, which form discrete lighter and darker bands. The white arrow in Fig. 24c-d shows the thickest silt layer that subtly fines upward into the fine silt and clay layer.

Interpretation

The interlaminated massive mudstone and clast rich layers are interpreted to be the result of alternating currents that were rich in clasts, i.e. calciturbidites. The current was probably small, or low in sediment concentration hence the thin alternating layers.

The interlamination forms when the sedimentation rate and the lower critical velocity are lower than the floccule ripples (Yawar & Schieber, 2017). The plane parallel laminations may be the result of the segregation of the coarse silt from the fine silt and clay floccule mix while being transported near bed by a weak current. The subtle fining upward from the silt layer pointed by the arrow could be from a waning flow.

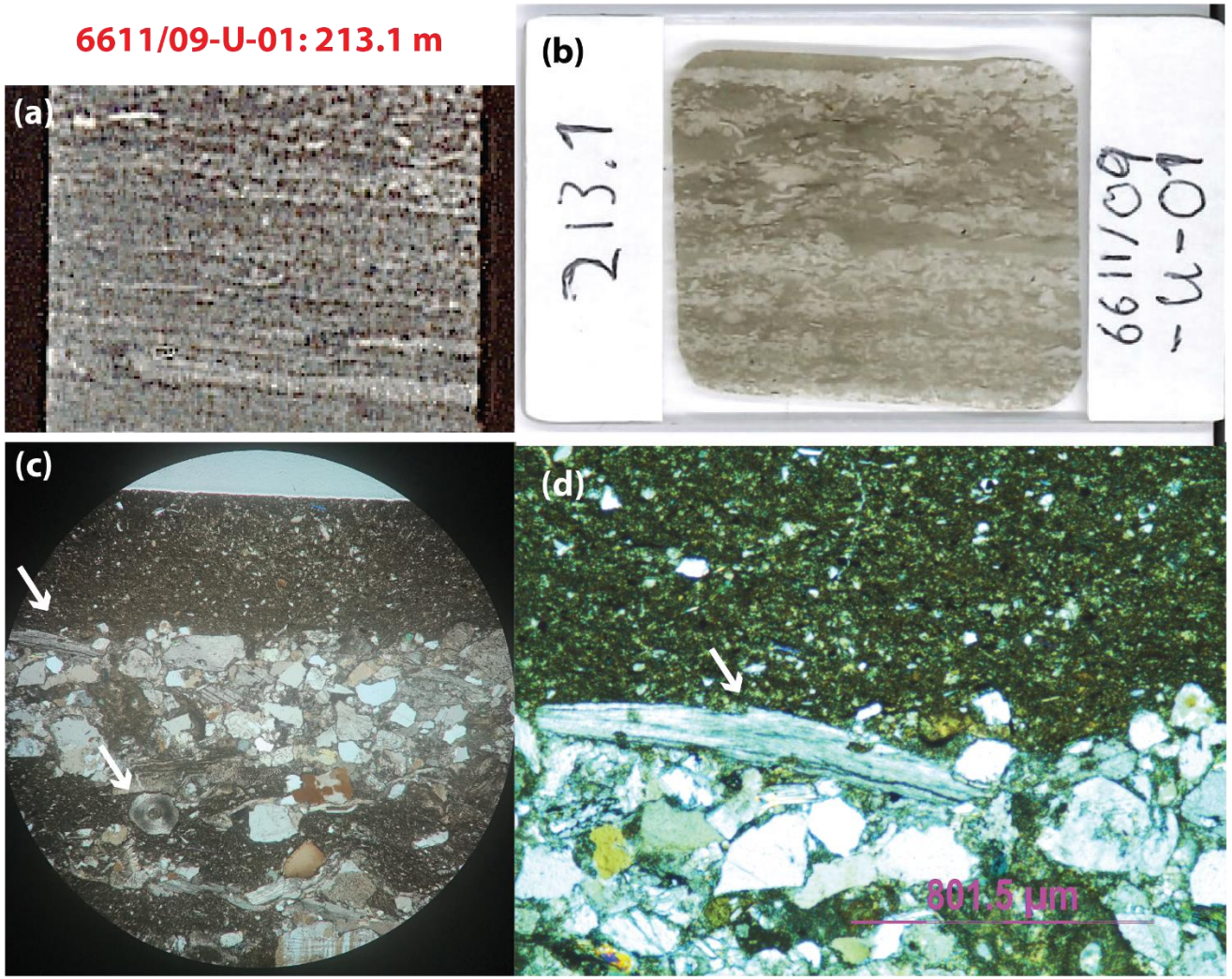

Fig. 23: Calciturbidites, interlaminated mudstone and calcareous fossil rich layers (a) core photo of the section (depth interval 213.1 m – 213.15 m), (b) full thin section scan, (c) shell fragment and ooids pointed at by the arrows, with magnification of 5x, field of view = 3.6 mm, (d) interbedded mud and fossil rich layers.

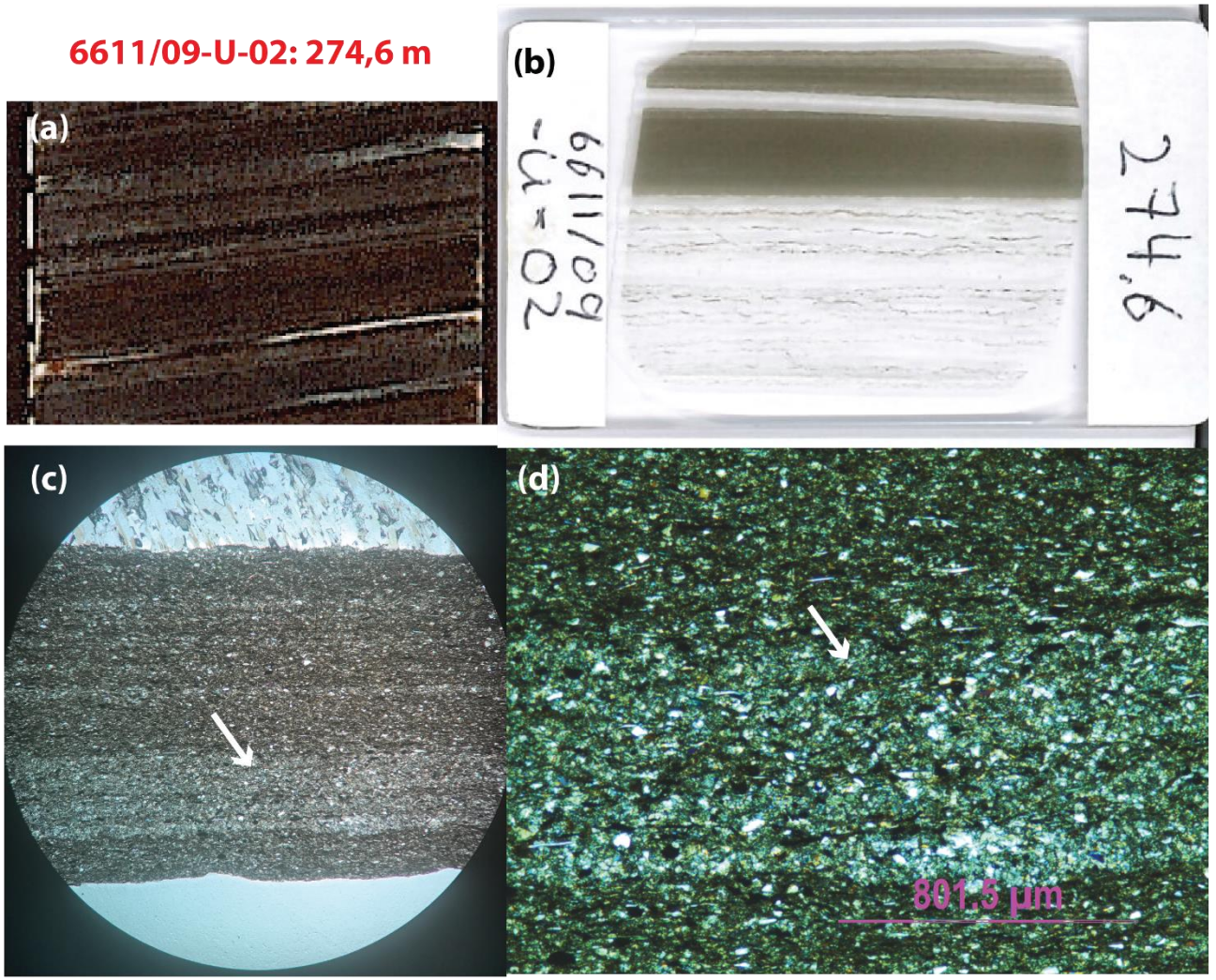

Fig. 24: Parallel laminated mudstone composed of interlaminated silt layers and fine silt/clay layers (a) core photo of the section (depth interval 274.6 m – 274.65 m), (b) full thin section scan, (c) parallel interlaminations with magnification of 5x, field of view = 3.6 mm, (d) a subtle fining upward from coarse silt into fine silt pointed by the arrow.

Description

The massive mudstone facies shown in Fig. 25, Fig. 26, and Fig. 27 comprise of inhomogeneous mud with discontinuous coarse silt and clay clasts and/or layers. These discontinuous patches were observed to be scattered throughout the thin section, which makes the massive mudstone look inhomogeneous, even in the cores, although it is less visible in the core photograph due to the dark colour. The shapes of these clasts vary from elongated with a planar geometry such as in Fig. 25, to be more irregularly shaped such as in Fig. 26. In contrast to the other two thin sections, Fig. 27 shows much more complex layers which appear to be a disturbed planar lamination. This thin section also shows a subtle fining up from the silt-rich to the clay-rich part (Fig. 27b).

Interpretation

Massive sandstone can be produced from suspension settling, however flocculation can enhance the deposition. The mud clasts might be the result of erosion that subsequently gets redeposited together with the suspension settling of the mudstone (Yawar & Schieber, 2017). Inhomogeneous mudstone can be tricky as the original structures might have been destroyed or flattened, an SEM analysis would give a better result than thin section microscopy.

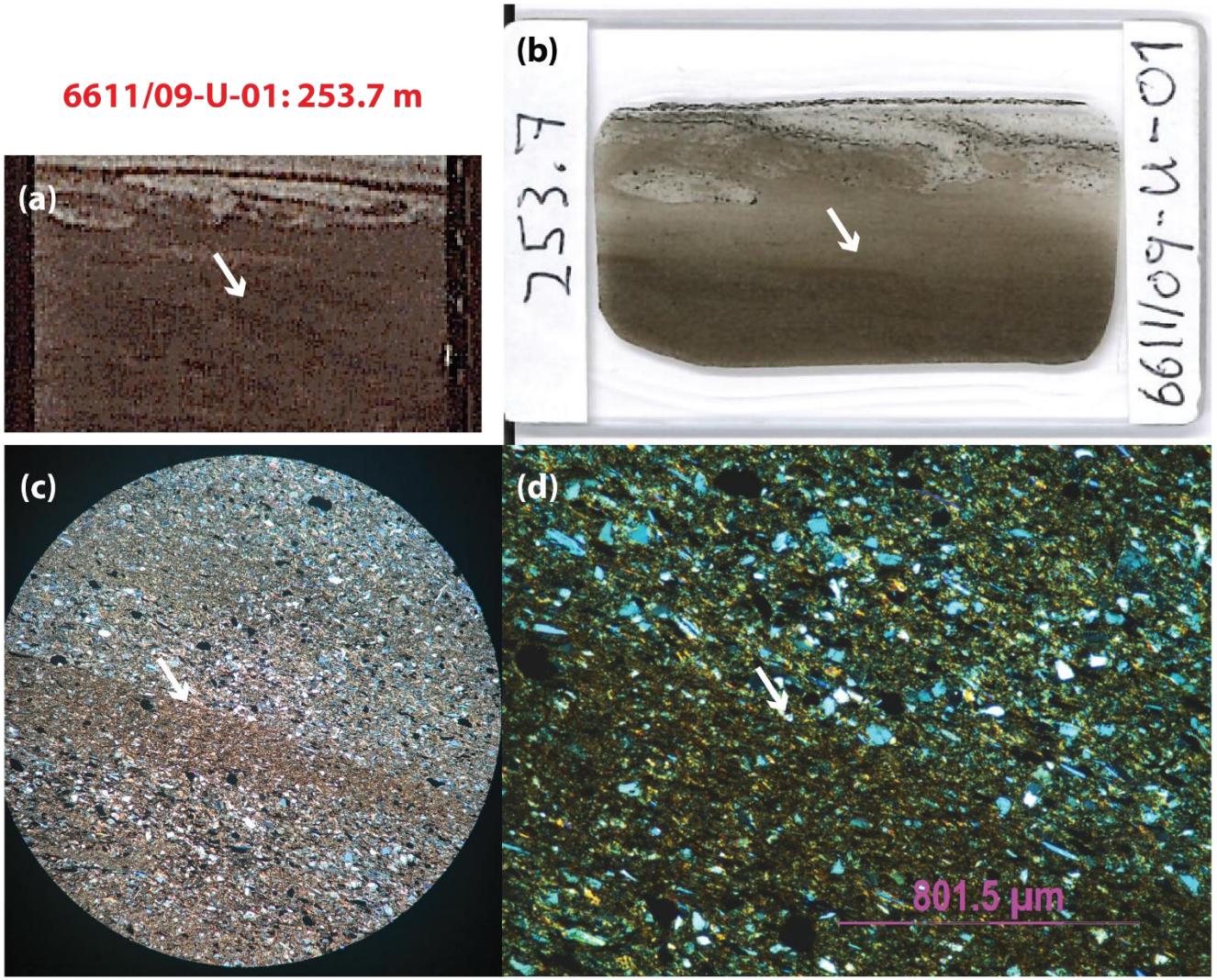

Fig. 25: Parallel laminated mudstone composed of interlaminated silt layers and fine silt/clay layers (a) core photo of the section (depth interval 274.6 m – 274.65 m); above the white arrow is a loading structure, (b) full thin section scan, (c) parallel interlaminations with magnification of 5x, field of view = 3.6 mm, (d) zoomed in version of the mud lamina.

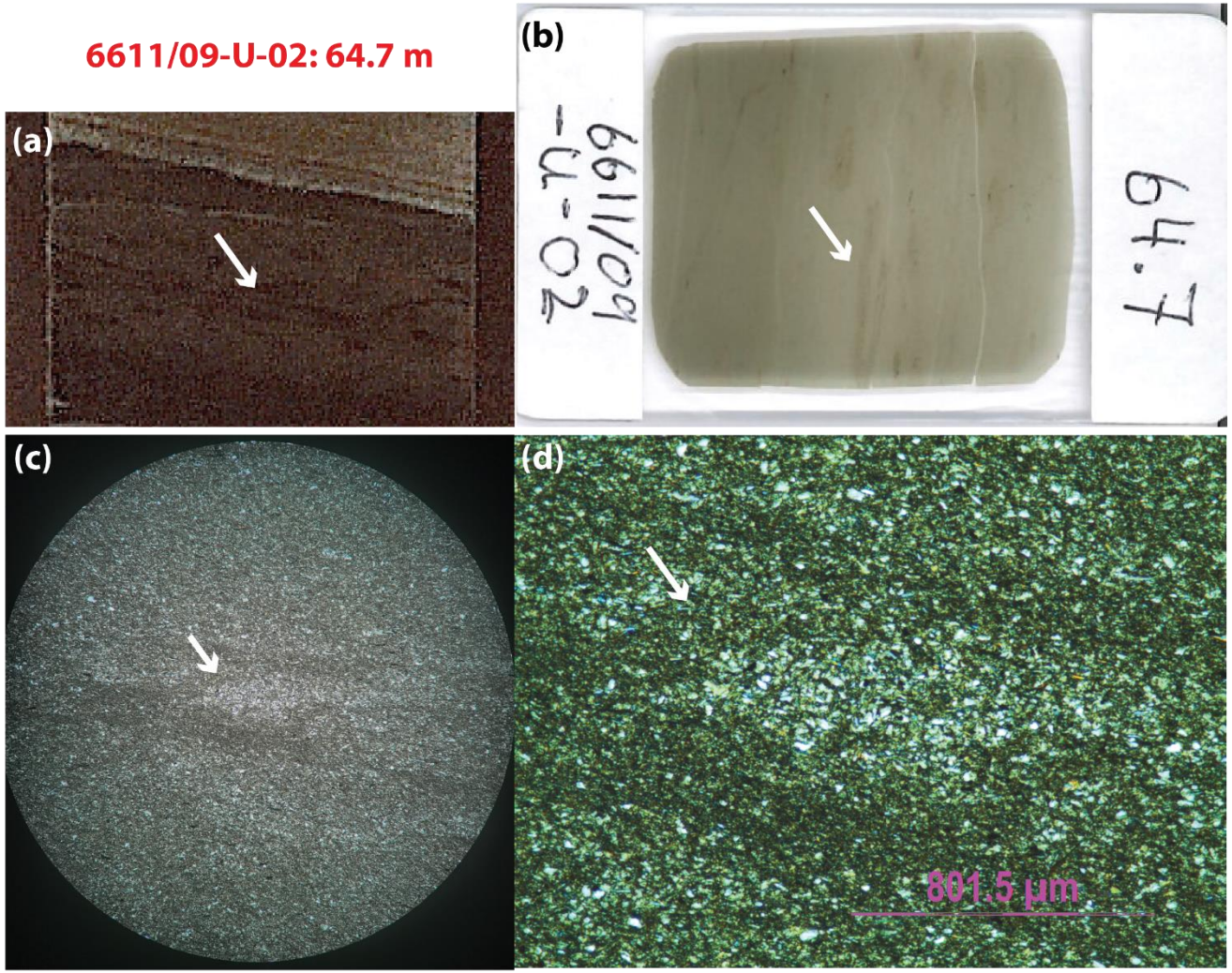

Fig. 26: Inhomogeneous mudstone showing discontinuous silt and mud layers (a) a core photo of the section (depth interval 64.7 m – 64.75 m), (b) full thin section scan, (c) inhomogeneous mudstone with magnification of 5x, field of view = 3.6 mm, (d) a silty, discontinuous lamina, with some fine materials below and above it.

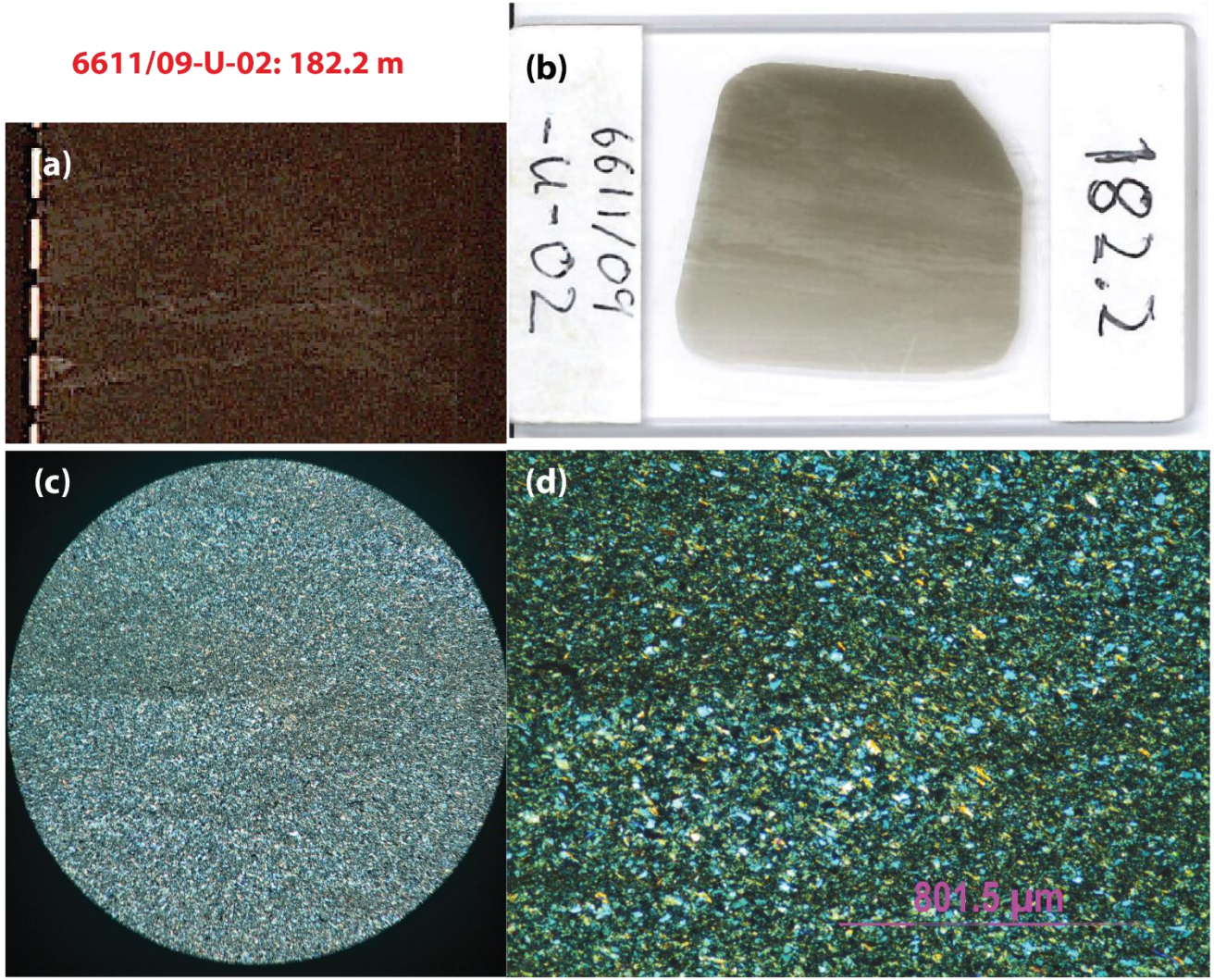

Fig. 27: Inhomogeneous mudstone showing discontinuous silt and mud layers (a) a core photo of the section (depth interval 182.2 m – 182.25 m), (b) full thin section scan, (c) inhomogeneous mudstone with magnification of 5x, field of view = 3.6 mm, (d) a silty, discontinuous lamina, with some fine materials below and above it.

3.3 SAND INJECTITES

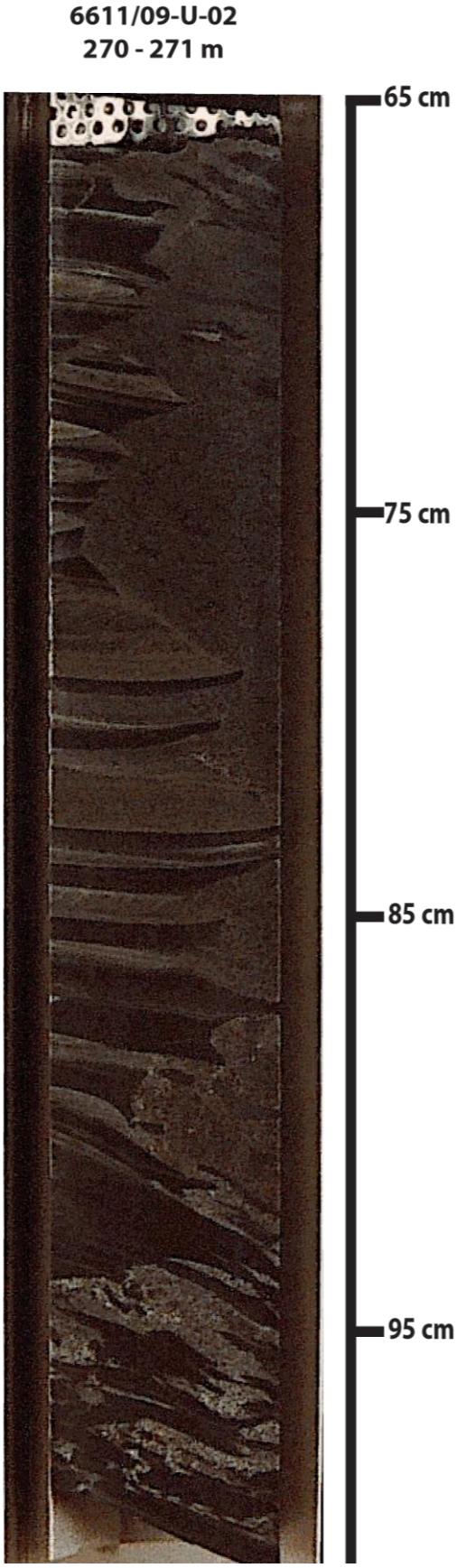

Sand injectites found in several intervals within the Turbidite Units are post-depositional structures caused by mobilised sand. The injectites are typically fine- to medium-grained sand and structureless. In the cores, the typical thickness is around 40 cm. The most defining features of sand injectites is their contact with the host beds; commonly discordant to the bedding angles and with irregular contacts, where the grains are observed to be aligned parallel to the contact. Fig. 28 shows an example of sand injectites that disrupted the thin interbedded sandstone-mudstone facies. In this case, the sand injectite is very clear due to contrasting facies. This type of sand injectite that intruded laterally or horizontally is called sandstone sill (Hurst et al., 2011).

The remobilisation is caused by liquefaction or fluidization due to high pore fluid content, which under external force will try to escape (Allen, 1985; Hurst et al., 2011). According to Haughton et al. (2009), sand injectite could also be linked to a hybrid bed where it's sourced from the underlying, dewatering sandstone bed.

Fig. 28: Core photo showing sand injectite of medium sandstone intruding into interbedded sandstone-mudstone interval. The contact with the host bed is discordant and wavy. From core 6611/09-U-02, depth interval 270 m – 271 m. The depth intervals are measure from top downward for each 1 metre long core, measurement on the side of the photos indicate 10 cm intervals downward (1 – 100 cm).

3.4 FACIES ASSOCIATIONS AND FLOW MODELS

A facies association is defined here as one or more depositionally related facies. They are described from low to high density, from most transformed to least transformed. The lower and upper contacts are important in determining the facies associations. These contacts can be sharp or gradual. A sharp contact is defined by an abrupt change in grain size and texture, and can be an erosional contact. It often indicates a break or the termination of a single flow process. On the other hand, a gradual contact does not indicate a break, but rather a continuous deposition from the same parent flow, such as that of the gradually fining upward succession of Bouma T_a - T_e. Each facies association corresponds to a single flow process, illustrated here as the flow models.

Low density turbidite

Low density turbidites display 2 to 4 divisions showing a gradual fining up sequence of: fining upward sandstone, planar laminated sandstone, ripple sandstone and mudstone. The mudstone is typically thin, either massive or laminated. There are few variations to the sequences as illustrated in Fig. 29 below. The overall fining upward trend is characteristics of a low concentration, non-cohesive, decelerating turbidity current (e.g. Collinson et al., 2006). The typical facies association is shown in Fig. 30.

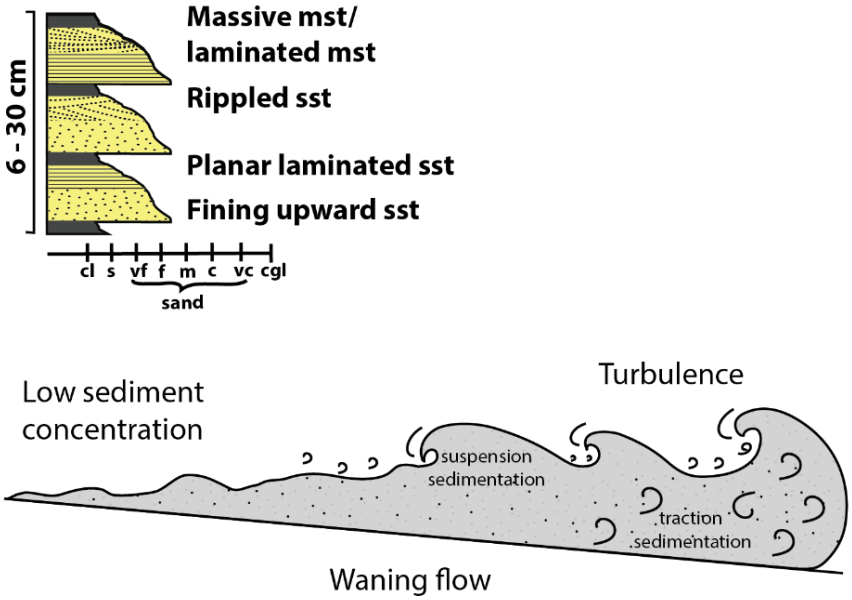

Fig. 29: Diagram showing the facies association and flow process of a low-density turbidity current.

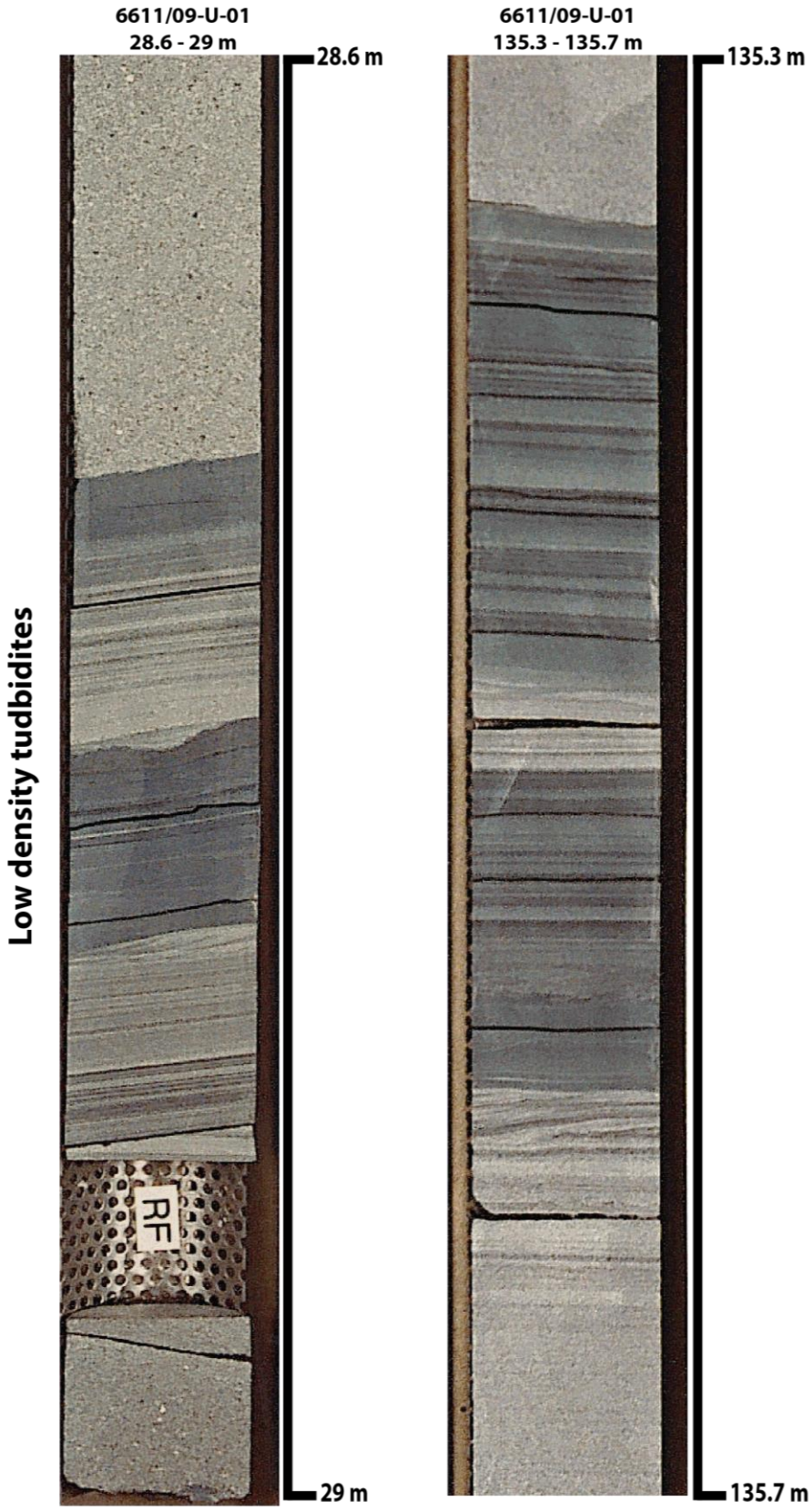

Fig. 30: Core photos showing facies association of a low density turbidite.

High density turbidite

The high density turbidite facies association is characterized by thick massive sandstone facies at the base of the flow, occasionally with presence of pebbles. The sequence continues into fining upward sandstone, sandstone with tractional features and finally capped with mud. This sequence is typical of Lowe's high-density turbidity current with higher sediment concentration compared to the low-density turbidity current (Lowe, 1982). Fig. 31 shows the highest sediment concentration is found near bed where the shear rate is the highest (Lowe, 1982), where it is possible to have relatively rapid deposition as the turbidity current progressively loses its capacity (Hiscott, 1995).

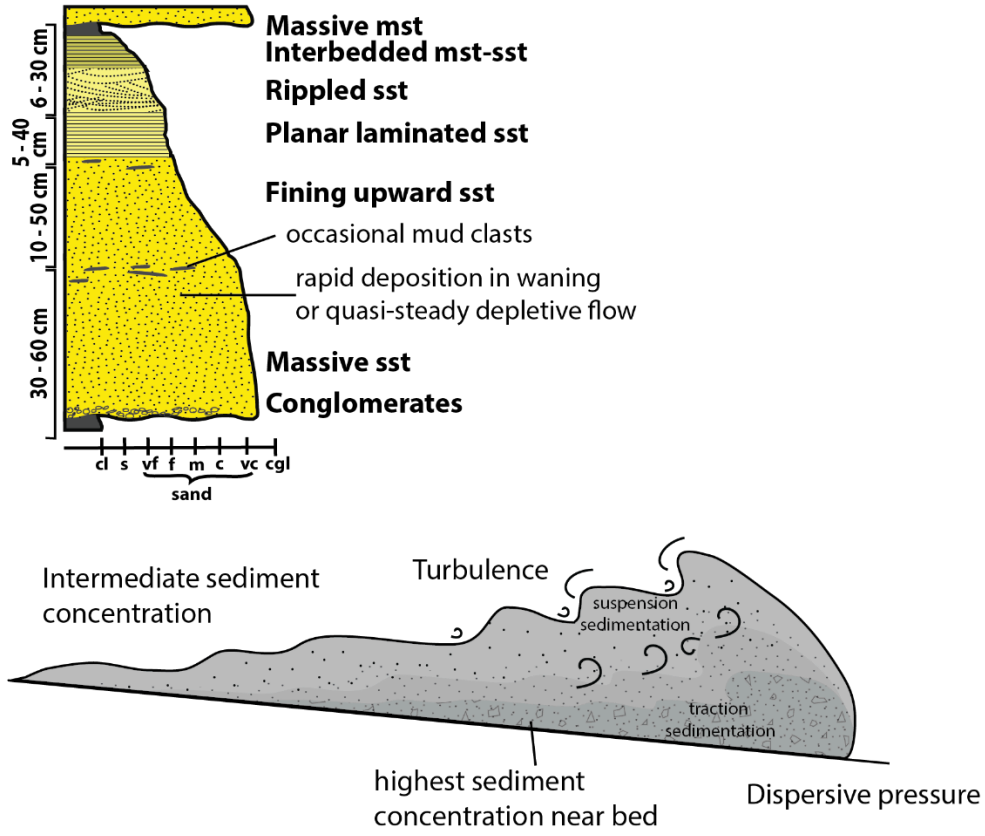

Fig. 31: Diagram showing the facies association and flow process of a high-density turbidity current.

Fig. 32: Core photos showing facies association of a high density turbidite. Core photos showing the whole 1 metre section where the facies association occurred.

Mudflow

Mudflow deposits display mud-rich divisions such as sandy mudstone facies, laminated mudstone facies and massive mudstone facies. This muddy deposit is characteristic of a cohesive flow that is deposited via cohesive freezing. Fig. 33 illustrates most of the sediment is transported via suspension where the coarse grains supported by the muddy fluid. Mudflow is the least concentrated flow compared to the other cohesive flows as observed in the floating coarse grains (sand and pebbles). The contact between the facies is gradual and the overall appearance is dark grey. The typical appearance of this facies association can be seen in Fig. 18b.

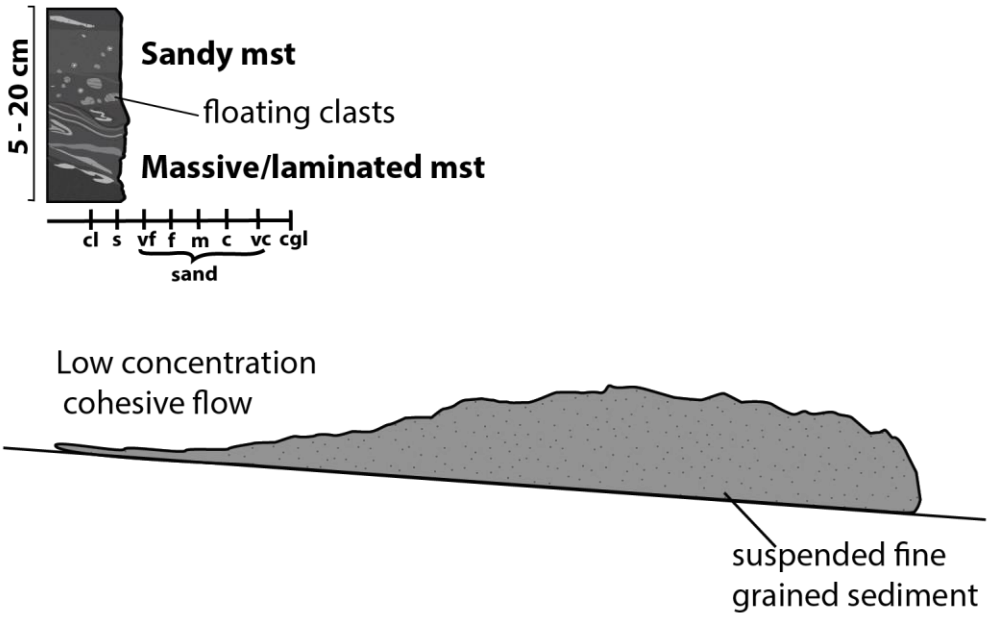

Fig. 33: Diagram showing the facies association and inferred flow process of a mud flow.

Debrite

Debrite can be subdivided into two divisions from base to top as: muddy sandstone which gradually transitions into a chaotic bed with a sharp top. The chaotic fabric is indicative of laminar flow that is deposited by cohesive freezing. The sandy mudstone is sheared, whilst the mud clast rich top of the chaotic facies is indicative of a plug flow within the debris flow. The typical appearance of this facies association is shown in Fig. 13.

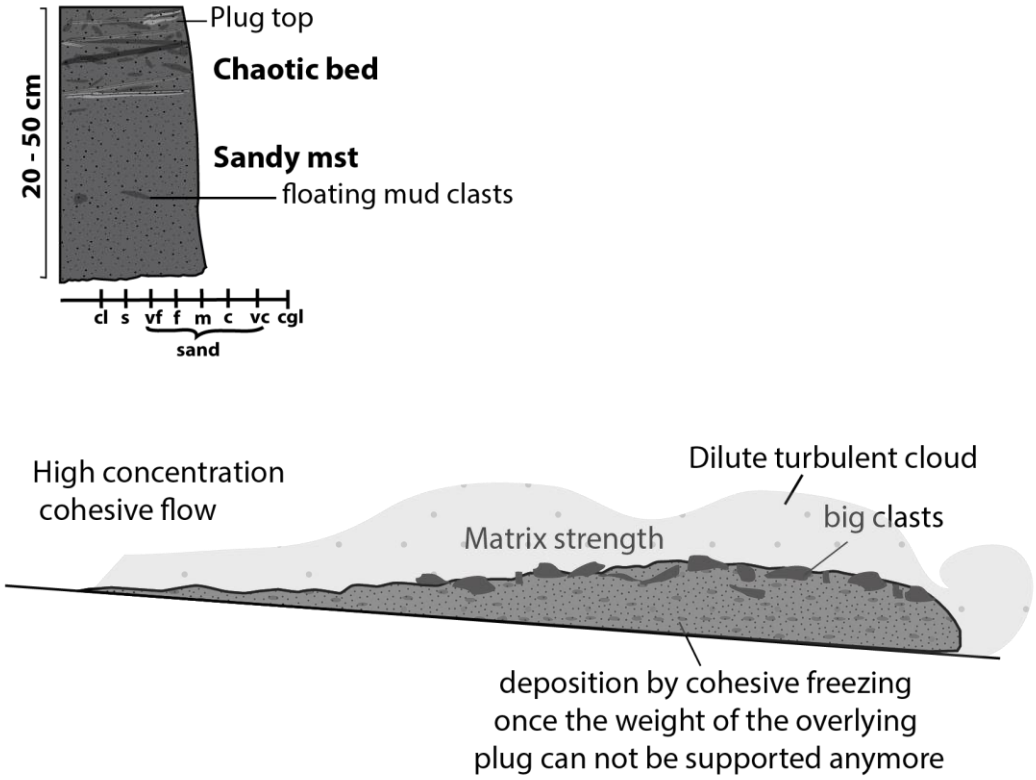

Fig. 34: Diagram showing the facies association and inferred flow process of a debris flow.

Slump and slide

Both a slump and a slide represent a coherent body that has been sheared. They can be recognized from the presence of original bedding that is still recognisable. Slumps were found here to have distorted heterolithic layer that have sharp lower and upper contacts with the other facies. The distorted layers are evenly sheared as illustrated in Fig. 35. Slides are characterised by the clearer original bedding compared to slumps, and contains a lot of micro faults that indicate translation and shearing of the layers (Fig. 36). The typical appearance of this facies association is shown in Fig. 37.

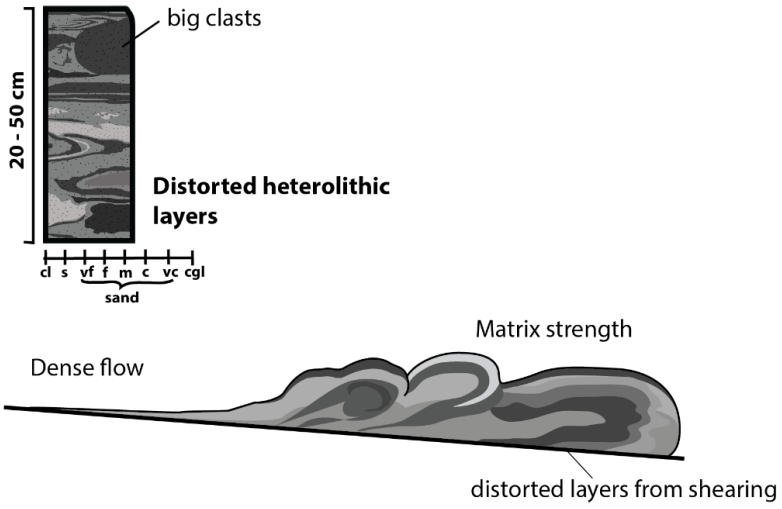

Fig. 35: Diagram showing the facies association and inferred flow process of a slump.

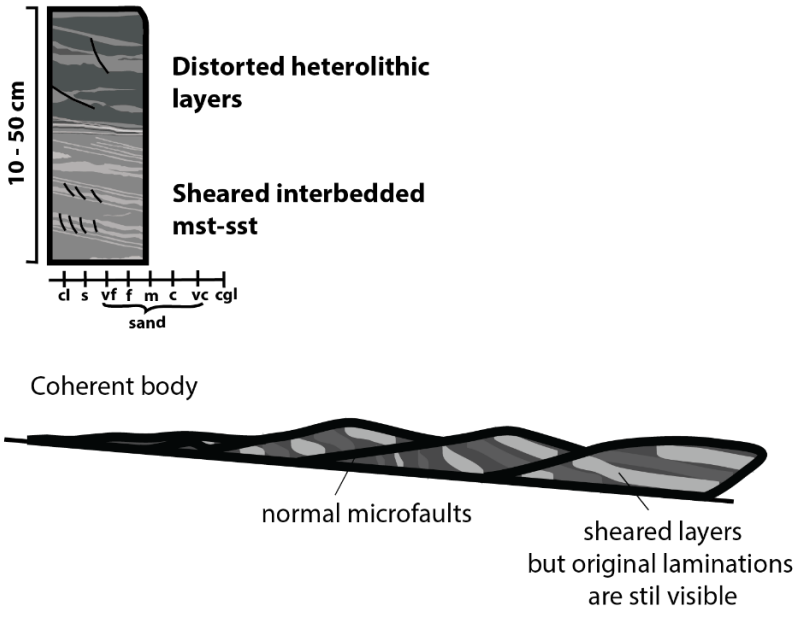

Fig. 36: Diagram showing the facies association and inferred flow process of a slide.

Fig. 37: Core photos showing facies associations of slump and slide.

Debrite encased in low density turbidites

According to the classification by Felix et al. (2009), this facies association would fit into a high strength with erosional top dense flow (Fig. 38). The transformation of a debris flow with high material strength is characterized by presence of low density turbidites below and above a debrite. The base often has a thin, turbidite sandstone that gradually change into a debritic facies with the chaotic facies at the top. The debrite is often capped by thin deposits showing tractional structures such as laminated sandstone, or ripple sandstone, and mudstone as illustrated in Fig. 38. The low density turbid cloud is formed by the erosion on the top of the debris flow. The basal sand is deposited from a dilute turbulent head from the erosion of the debris flow that detaches and runs ahead of the main flow Once the debris flow freezes, the leftover turbid cloud then forms a low-density turbidity current. Typical appearance of this facies association is shown in Fig. 40.

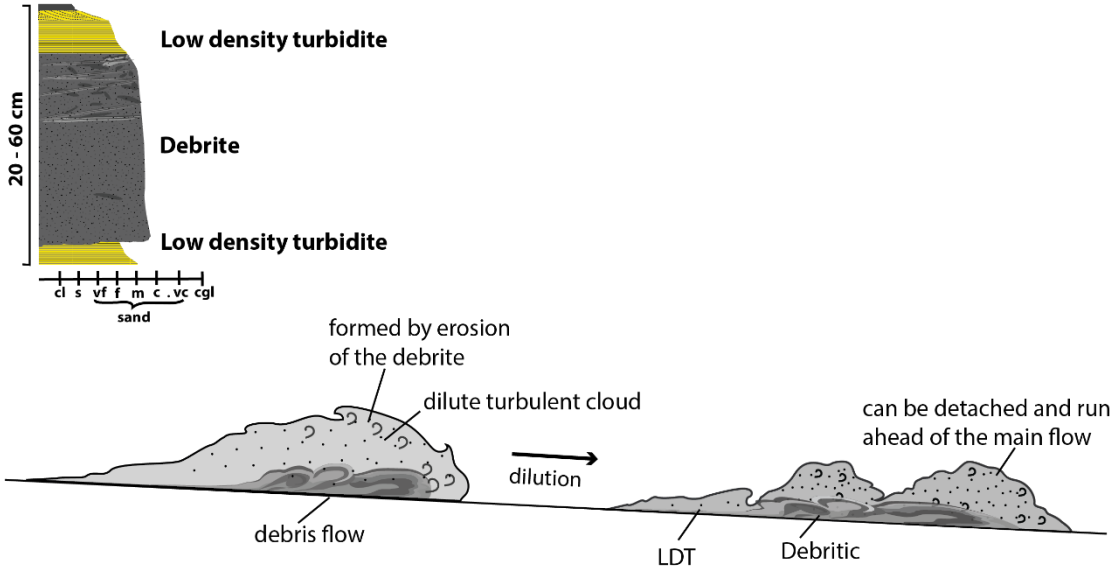

Fig. 38: Diagram showing the facies association and inferred flow process of a dense to dilute flow transformation

Alternating dense material and mixed debrite

This facies association is part of an intermediate strength dense flows that has multiple parts (Fig. 39). The intermediate material strength is characterized by different facies associations because the transforming flow would have laterally different parts (Felix & Peakall, 2006). In general, the deposit would record a complex alternation of mud-poor and mud-rich intervals, often with parts of the dense material too. The division often starts with a patchy

sandstone that gradually transitions into a sandy, chaotic bed that continues into distorted heterolithic bed. The heterolithic bed is often accompanied by patchy sandstones that alternates with muddy sandstone, as shown in Fig. 39. The contacts between the facies are often sharp, but at an angle to the normal bedding that indicate that the facies are deposited together. The typical appearance of this deposit is shown in Fig. 41.

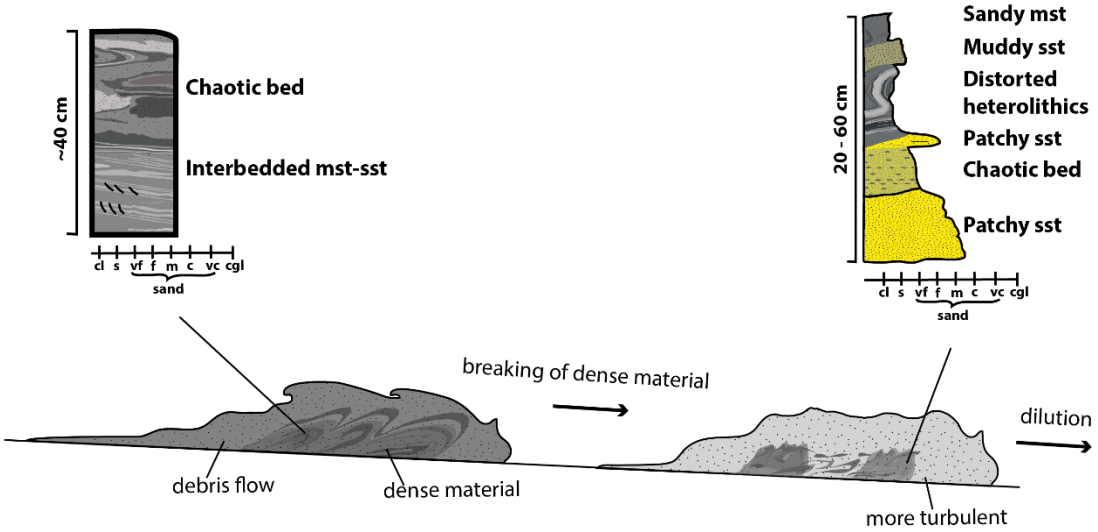

Fig. 39: Diagram showing the facies association and inferred flow process of a dense to dilute flow transformation

The alternating facies is the result of vertical and lateral variation in the transforming flow, where the distorted heterolithic facies is the dense material still preserved in the flow, and the patchy sandstone is the fully mixed part. The patchy sandstone is very indicative in this flow transformation as it characterises the last stages of dense to dilute flow transformation. Both debrite encased in low density turbidites and alternating dense material and mixed debrite are part of the dense to dilute transformation.

Fig. 40: Core photos showing facies association of a debrite encased in low density turbidite (LDT).

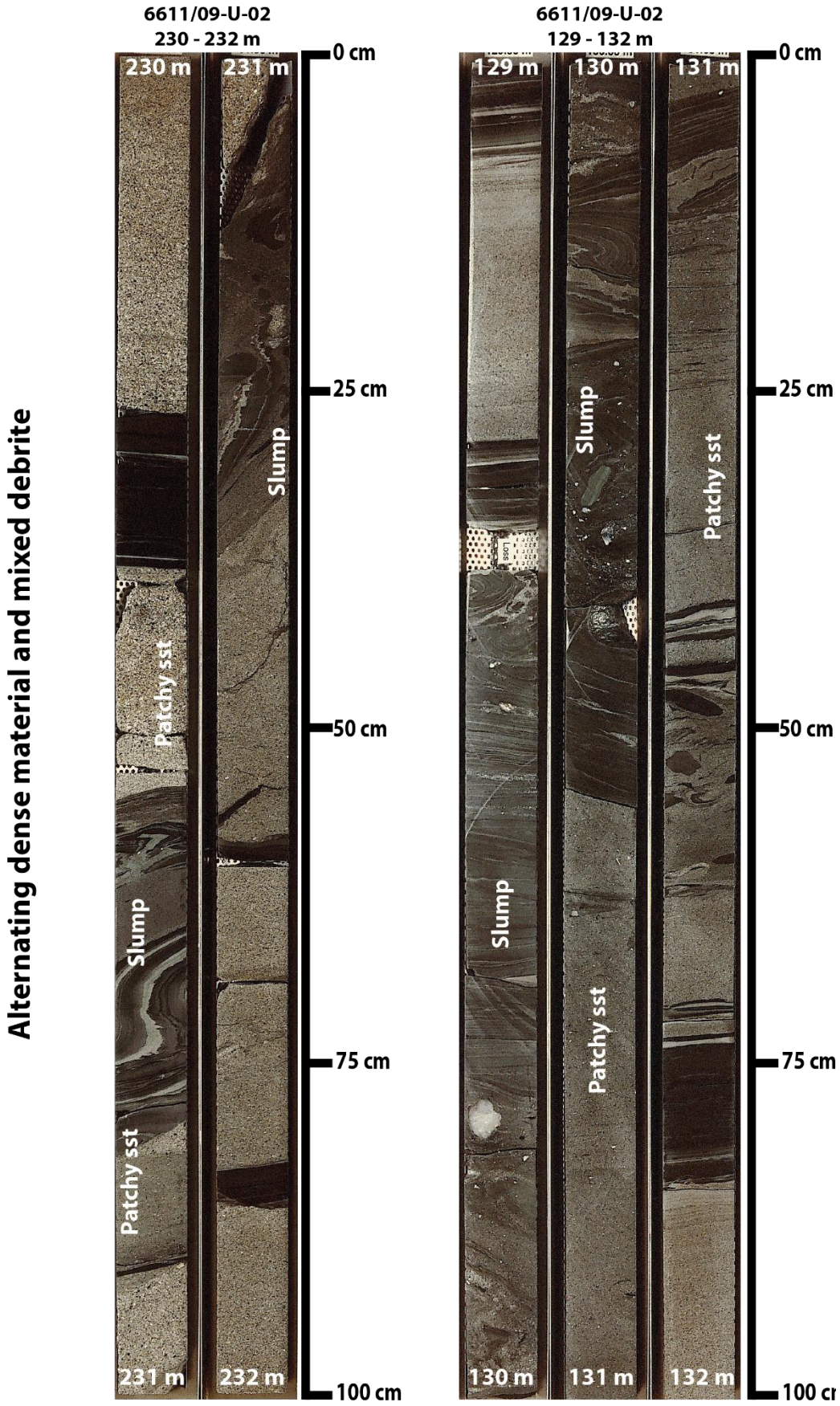

Fig. 41: Core photos showing facies association of alternating dense material and mixed debrite. Core photos showing the whole 1 metre section where the facies association occurred.

High density turbidite – debrite couplet

This facies association consists of a thick (≥30 cm) massive sandstone facies overlain by chaotic facies, the contact is often sharp (often sheared) at an angle to the normal bedding as shown in Fig. 42. The massive sandstone is indicative of aggradational deposition from turbidity current. The chaotic facies contains angular mud clasts, ranging from small (1 cm) to large, laminated mud clasts (>5 cm) and have a sharp top, which are the characteristics of en masse freezing from a debris flow. The sharp contact between the massive sandstone and the chaotic bed could indicate that the two facies were deposited separately, i.e. turbidite was deposited first followed closely by the debrite. It is similar to what has been described by Haughton et al. (2009) where the flow partitioned into two separate parts and deposited the massive sandstone (H1) and chaotic facies (H3).

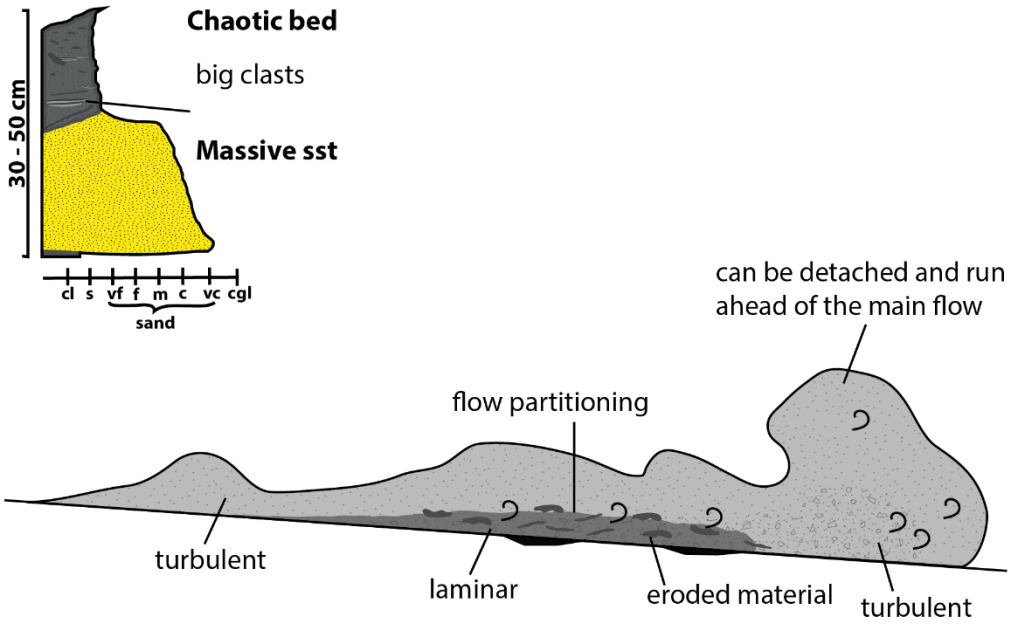

Fig. 42: Diagram showing the facies association and inferred flow process of a dilute to dense flow transformation

High density turbidite – debrite – low density turbidite

This facies association displays similar facies to the high density and debrite couplet, but it is capped by a thin, low density turbidite. The base is characterized by a clean, massive sandstone which gradually transition into muddy facies. The massive sandstone is often thick (≥30 cm). The muddy facies is either a chaotic facies or a muddy sandstone that contains both small (1 cm) and large angular mud clasts concentrated near the top. The chaotic facies

gradually transitions into a fining upwards sandstone that is typical of a low-density turbidity current, often showing tractional structures such as laminated sandstone as shown in Fig. 43. The overall appearance of this facies association is shown in Fig. 44.

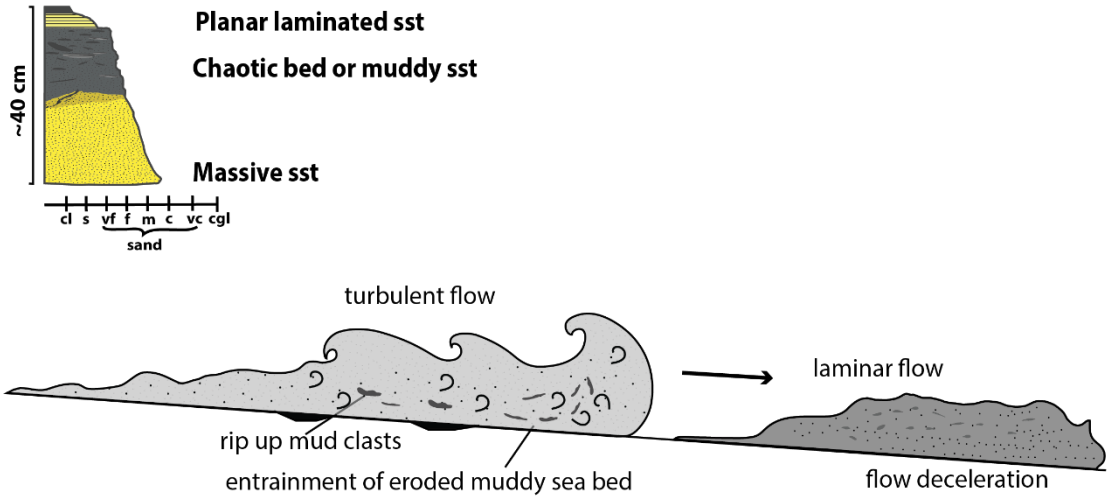

Fig. 43: Diagram showing the facies association and inferred flow process of a dilute to dense flow transformation

Both the high density turbidite – debrite and the high density turbidite – debrite – low density turbidite facies associations are the result of dilute to dense flow transformation. There is no presence no presence of patchy sandstone facies. The debrite here is similar to division H3 in Haughton et al. (2009). The thick basal sandstone that gradually changes into chaotic facies indicate that the flow is originally turbulent, then changed into laminar. The thin, low density turbidite cap could have been formed from a turbid cloud similar to division H4 from Haughton et al. (2009).

Fig. 44: Core photos showing facies association of debrite underlain by massive sandstone (high density turbidite/HDT) and overlain by low density turbidite (LDT)

4 DISCUSSION

Ten different flow types and their facies associations were interpreted from the results, where four facies associations show flow transformation: two from dense to dilute flow transformation and another two from dilute to dense flows transformation. The different types of flow transformation are classified according to the original concentration and composition of the parent flow. The type of facies that can be found in the deposits depends on the stage of flow transformation during which it was deposited. Essentially, the flow transformations observed are between different types of debris flow where not all sediment has been churned up completely yet, to more complete mixing and turbidity current. Here, the difference between the two flow transformation types will be discussed.

4.1 DENSE TO DILUTE FLOW TRANSFORMATION

The evidence of dense to dilute flow transformation have been observed in these cores as different facies associations, including a debrite with low density turbidites above and below it, and alternating mud-poor and mud-rich intervals. The former facies association indicates an early stage of the transformation or a dense flow with very high material strength that is not so easily eroded and mixed with the ambient fluid. Thus, the debris flows are often accompanied by low density turbidity currents generated by the erosion from the surface of the dense flows (i.e. shear with the surrounding water). The latter flow type contains broken pieces of the dense material within a mixed flow that indicate a later stage in the transformation.

In general, the defining characteristics of dense to dilute transformation can be summarised as having (1) large distorted heterolithic facies, and (2) patchy sandstone facies. In the early stages of the dense to dilute transformation, more of the distorted heterolithic facies should be present, as very little of the dense flow has undergone mixing. The dense flow would flow separately from the turbid cloud as a slump. As the dense flow breaks up with more mixing, the size of the distorted heterolithic clasts should decrease. At this stage, the dense material (previously slump) should be found alternating with other more mixed facies such as the patchy sandstone. The contact of the dense material and the patchy sandstone should be sharp, but at an angle to the normal bedding. This type of contact indicates shearing at the interface between the dense and the more dilute flow, where

erosion could take place. With further mixing and dilution, there should be less of the dense material preserved, and there should be more of the patchy sandstone facies.

The presence of patchy sandstone is important as it indicates one of the last stages of transformation whereby most of the dense material (especially the muddy parts) have been broken down, while the rounded sand clasts are still preserved. These rounded sand clasts cannot be the result of dilute to dense flow because the erosion of sand is grain-by-grain erosion and not in masses like mud beds (Allen, 1985). Moreover, sand does not have the ability to flocculate like clay particles thus will not be able to join up to form an aggregate during the transformation process. An alternative explanation to the patchy sandstone facies would be the result of syn-depositional sand injectites such as unit H3 in Haughton et al. (2009) classification. However, this seems unlikely for this case as the grains in the patchy sandstone are not aligned parallel to the contact with the host. Whereas in sand injectites, the grains are aligned parallel to the discordant contact with the host bed (Hurst et al., 2011).

4.2 DILUTE TO DENSE FLOW TRANSFORMATION

The transformation from dilute to dense flows is generally by the intake of dispersed clay into the flow and subsequent deceleration of the flow. The dispersed clay can dampen turbulence; hence the resulting deposits generally display a gradual transition from turbiditic facies into debritic facies (Haughton et al., 2003; Baas et al., 2009). This facies does not have patchy sandstone facies; as previously explained, the rounded sand patches could not have formed by erosion of a sandy bed. In general, the characteristics of dilute to dense flow transformation include: (1) the base of the bed contains a turbidite which gradually transitions into debritic facies, (2) presence of rip up mud clasts (i.e. angular), and (3) a sharp top indicating an abrupt end, or gradual change from chaotic facies to a thin, low density turbidite cap.

The initiation of flow transformation depends on the condition and behaviour of the basin, e.g. dilute to dense flow transformation needs an erodible muddy sea bed, thus, the basin condition influences the amount of clay that will be incorporated into the flow to generate dilute to dense flow transformation. The erosion of muddy seabed depends on the degree of compaction it has undergone, where semi-lithified mudstone erodes in chunks

(e.g. Haughton et al., 2009) whilst uncompacted water-rich mud erodes as small rip-up clasts due to lack in shear strength (Einsele et al., 1974). Schieber et al. (2010) demonstrated erosion of water-rich mudstone in their experiment which resulted in small (millimetre to sub millimetre sized) rip up clasts. The rip up mud clasts from the water-rich layers were observed to be broken up and reduced in size as they get transported, indicating that dispersed clay would be available in the transforming flow (Schieber et al., 2010) to change its flow regime from turbulent into transitional or laminar flow (Baas et al., 2009). In contrast, the semi-lithified mudstone would be more difficult to quickly break down and be resuspended as dispersed clay. This means that the frequency of dilute to dense flow transformation depends on the availability of the water-rich muds. To accumulate a significant amount of the water-rich muds, the basin condition needs to be somewhat quiescent, otherwise they would always be eroded, broken down, and resuspended.

The injection and delamination mechanism suggested by Fonnesu et al. (2016) include the erosion of a large raft (2-20 m) which is even more difficult to break down than rip up mud clasts. This mechanism would be less likely to actually dampen the turbulent parent flow and change the flow into transitional or laminar flow.

4.3 SUMMARY: HOW TO DIFFERENTIATE WHICH TYPE OF FLOW TRANSFORMATION?

Flow transformation is a continuum process that changes one type of sediment gravity flow to another through progressive stages. The resulting deposits represent parts of the continuum that are sometimes vague and difficult to interpret, as different mechanisms may produce similar deposits. Overall, the determination of facies association and vertical relationship between the facies are important tools to interpret the origin of the deposits.

In the deposits, the most distinguishing characteristics of dense to dilute flow transformation, from early (proximal) to late (distal) are the presence of slumps that alternate with patchy sandstone. On the other hand, in dilute to dense flow transformation, the basal (often massive) sandstone that gradually changes into chaotic bed is indicative of a turbulent parent flow that changes into a laminar flow. Fig. 45 summarizes all the possible flow transformations of both end-members, along with the mechanisms. The diagram illustrates how flow transformation might be more common than what has been thought, as it involves a spectrum of different flow types. The characteristics as to tell which flow transformation a deposit represents are summarized in Fig. 46 based on the inferred mechanisms. Finally, a single sediment gravity flow can undergo multiple flow transformations, thus further complicating the final deposits.

Different stages of flow transformation and their mechanisms

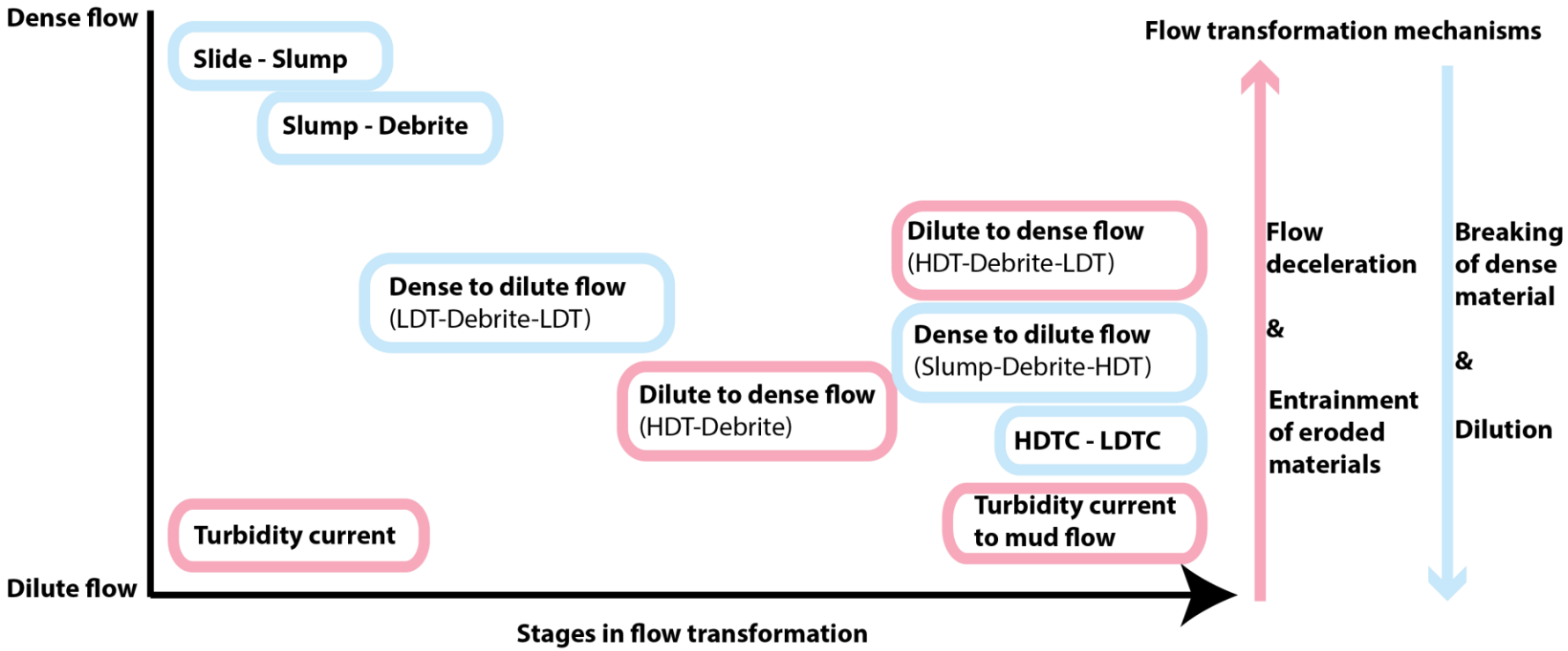

Fig. 45: Summary of the different stages in both end-members of the flow transformation. The blue boxes and arrow show dense to dilute flow transformation, while the pink boxes and arrow show dilute to dense flow transformation. The boxes showing common flow transformations in bold, and the expected deposits in the brackets. LDT = low density turbidity, HDT = high density turbidite, LDTC = low density turbidity current, HDTC = high density turbidity current.

Stage characteristics of flow transformation

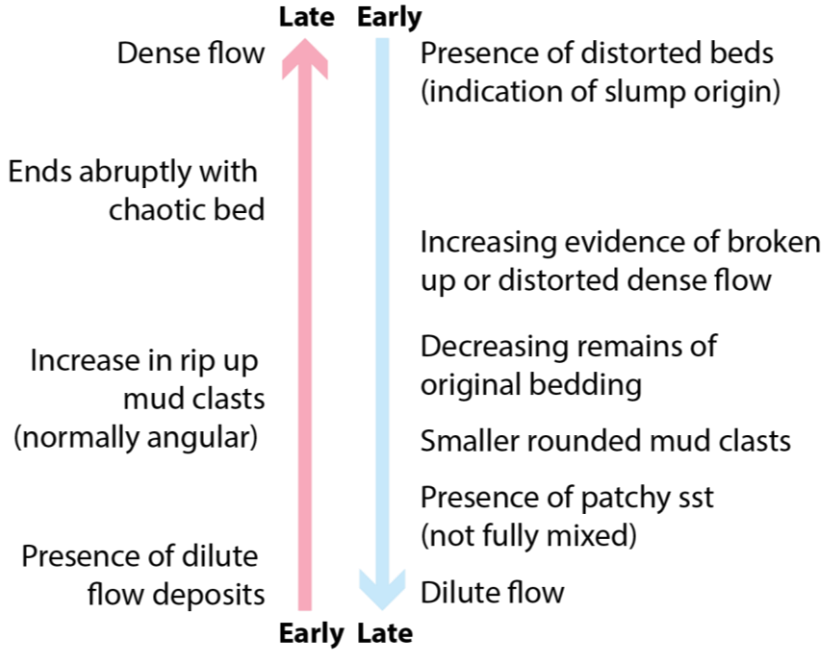

Fig. 46: Summary of the deposit characteristics of the two end-members of the flow transformation. Blue arrow shows dense to dilute flow transformation, and pink arrow shows dilute to dense flow transformation.

4.4 ENVIRONMENTAL SETTINGS

Most of the muddy interval has been interpreted as formed in a quiescent environment during periods of anoxia (Bugge et al., 2002). What is often overlooked is the fact that ancient mudstones have undergone compaction that reduced a great amount of their original thickness. In other words, any structures formed previously may be destroyed or flattened. Some of these microstructures may be more common than previously thought within the mud portion of sediment gravity flow deposits, that could indicate the basin condition under which the transforming flow formed from.

From the thin section study, it was found that all of the laminated mudstone have microstructures, including ripples, planar laminations, normal grading, and the massive mudstone is inhomogeneous probably with rip up mud clasts. Although there were limited thin sections, these microstructures are expected to occur throughout the whole cores where the same laminated and massive mudstone facies occur. This concludes that the environment in which muds deposit might not be as quiescent as has been interpreted by Bugge et al. (2002), and that muds can form structures just like sand.

The presence of microstructures in the mudstones can indicate a rather active environment, because ripples and erosion occur at critical velocity of 25 cm/s (Schieber et al., 2010; Yawar & Schieber, 2017). If this is true, then the condition of the basin was quite active where there were a lot of gravity flows eroding the freshly deposited mud, thus the basin probably had less water-rich clays. Therefore, most of the dilute to dense transformation is from the incorporation of mud clasts, which indicate longer transport is needed to change these clasts into dispersed mud as compared to the incorporation of water-rich clays.

5 CONCLUSION

Flow transformation and its mechanisms had been described separately as two end-members: (1) dense to dilute flow, and (2) dilute to dense flow. In this study, the flow transformation is looked at a continuum process that changes one type of sediment gravity flow to another through progressive stages. The resulting deposits represent parts of the continuum that are sometimes vague and difficult to interpret, as different mechanisms may produce similar deposits. In this study, the distinguishing characteristics of each end-members have been described as a progressive change from early (proximal) to late (distal). For dense to dilute flow transformation, the progressive change is from a slump like deposit, to alternation of slump and patchy sandstone, and finally the presence of turbiditic deposit. For dilute to dense flow transformation, the progressive change is from a basal massive sandstone that gradually changes into chaotic bed, which is indicative of a turbulent parent flow that changes into a laminar flow. In addition, the mudstones observed in this study is inferred to have formed by currents that erode and produce microstructures, which indicate a more active environment that what has been previously interpreted before.

References

Allen, J.R.L. (1985) *Principles of Physical Sedimentology*. London: Chapman & Hall, 272pp.

Amy, L. A., and Talling, P. J. (2006). Anatomy of turbidites and linked debrites based on long distance (120× 30 km) bed correlation, Marnoso Arenacea Formation, Northern Apennines, Italy. *Sedimentology*, **53** (1), 161-212.

Baas, J. H., Best, J. L., Peakall, J., and Wang, M. (2009). A phase diagram for turbulent, transitional, and laminar clay suspension flows. *J. Sed. Res.,* **79**(4), 162-183.

Bugge, T., Ringas, J., Leith, D., Mangerud, G., Weiss, H., and Leith, T. (2002). Upper Permian as a new play model on the mid-Norwegian continental shelf: Investigated by shallow stratigraphic drilling. *AAPG Bull*., **86** (1), 107-127.

Collinson, J., Mountney, N., and Thompson, D. (2006). *Sedimentary Structures*. Harpenden, Hert.: Terra, 304pp.

Doré, A. (1991). The structural foundation and evolution of Mesozoic seaways between Europe and the Arctic. *Palaeogeogr. Palaeoclimatol. Palaeoecol*. **87** (1-4): 441-492.

Einsele, G., Overbeck, R., Schwarz, H.U., and Unsold, G., 1974, Mass physical properties, sliding and erodability of experimentally deposited and differently consolidated clayey muds: *Sedimentology*, **21**, 339–372.

Faleide, J. I., Bjørlykke, K., and Gabrielsen, R. H. (2010). Geology of the Norwegian continental shelf. In: *Petroleum Geoscience: From Sedimentary Environments to Rock Physics* (Ed. K. Bjorlykke), Springer, Berlin. 603-637.

Felix, M., and Peakall**, J.** (2006). Transformation of debris flows into turbidity currents: mechanisms inferred from laboratory experiments. *Sedimentology,* **53** (1), 107-123.

Felix, M., Leszczyński, S., Ślączka, A., Uchman, A., Amy, L., and Peakall, J. (2009). Field expressions of the transformation of debris flows into turbidity currents, with examples from the Polish Carpathians and the French Maritime Alps. *Mar. Petrol. Geol.* **26** (10), 2011-2020.

Fonnesu, M., Patacci, M., Haughton, P. D., Felletti, F., and McCaffrey, W. D. (2016). Hybrid event beds generated by local substrate delamination on a confined-basin floor. *J. Sed. Res.,* **86** (8), 929-943.

Hallan, E.K., Gjeldvik, I.T., Johansen, W.T., Magnus, C., Meling, I.M., Mujezinovic, J., Riis, F., Rød, R.S., Pham, V.T.H., and Tappel, I. (2014). Structural elements in the Norwegian Sea [Image]. Retrieved April 12th, 2018 from http://www.npd.no/Global/Norsk/3-Publikasjoner/Rapporter /CO2-samleatlas/Chapter-5.pdf

Hand, B.M. (1997). Inverse grading resulting from coarse-sediment transport lag: *J. Sed. Res.,* **67** (1), 124-129.

Haughton, P. D., Barker, S. P., and McCaffrey, W. D. (2003). 'Linked' debrites in sand-rich turbidite systems–origin and significance. *Sedimentology*, **50**(3), 459-482.

Haughton, P., Davis, C., McCaffrey, W., and Barker, S. (2009). Hybrid sediment gravity flow deposits – classification, origin and significance. *Mar. Petrol. Geol.* **26**, 1900-1918.

Hiscott, R.N. (1994). Loss of capacity, not competence, as the fundamental process governing deposition from turbidity currents: *J. Sed. Res.,* **A64** (2), 209-214.

Hiscott, R.N. (1995), Traction carpet stratification in turbidites - fact or fiction? Reply*: J. Sed. Res.*, **A65**(4), p. 704-705.

Hurst, A., Scott, A., and Vigorito, M. (2011). Physical characteristics of sand injectites. *Earth-Sci. Rev*., **106** (3-4), 215-246.

Kneller, B.C., and Branney, M.J. (1995). Sustained high-density turbidity currents and the deposition of thick massive sands. *Sedimentology*, **42**, 607-616.

Kneller, B. C., and McCaffrey, W. D. (2003). The interpretation of vertical sequences in turbidite beds: the influence of longitudinal flow structure. *J. Sed. Res.*, **73** (5), 706-713.

Lowe, D. R. (1979). Sediment gravity flows: their classification and some problems of application to natural flows and deposits. *SEPM Spec. Publ.,* **27**, 75-82

Lowe, D.R. (1982). Sediment gravity flows II. Depositional models with special reference to the deposits of high-density turbidite currents. *J. Sed. Petrol.*, **52** (1), 279-297.

Osmundsen, P. T., Sommaruga, A., Skilbrei, J. R., and Olesen, O. (2002). Deep structure of the Mid Norway rifted margin. *Nor. J. Geol.* **82** (4), 205-224.

Pickering, K., and Hiscott, R. (2016). *Deep-marine systems: processes, deposits, environments, tectonics and sedimentation*. Chichester: Wiley-Blackwell. 672pp.

Schieber, J., Southard, J., and Thaisen, K. (2007). Accretion of mudstone beds from migrating floccule ripples. *Science*, **318**, 1760-1763.

Schieber, J., Southard, J. B., and Schimmelmann, A**.** (2010). Lenticular shale fabrics resulting from intermittent erosion of water-rich muds – interpreting the rock record in the light of recent flume experiments. *J. Sed. Res.*, **80**, 119–128.

Surlyk, F., Hurst, J. M., Piasecki, S., Rolle, F., Scholle, P. A., Stemmerik, L., and Thomsen, E. (1986). The Permian of the western margin of the Greenland Sea--a future exploration target. *AAPG Mem.*, **40**, 629-659

Talling, P. J., Amy, L. A., Wynn, R. B., Peakall, J., and Robinson, M. (2004). Beds comprising debrite sandwiched within co-genetic turbidite: origin and widespread occurrence in distal depositional environments. *Sedimentology.* **51**, 163–194.

Talling, P. J. (2013). Hybrid submarine flows comprising turbidity current and cohesive debris flow: Deposits, theoretical and experimental analyses, and generalized models. *Geosphere*, **9**(3), 460-488.

Talling, P. J., Malgesini, G., and Felletti, F. (2013). Can liquefied debris flows deposit clean sand over large areas of sea floor? Field evidence from the Marnoso-Arenacea Formation, Italian Apennines. *Sedimentology*, ***60***(3), 720-762.

Yawar, Z., and Schieber, J. (2017). On the origin of silt laminae in laminated shales. *Sed. Geol.,* 360, 22-34.